

## **Distribution of different isoforms of Receptor Protein Tyrosine Phosphatase $\gamma$ (Ptp $\gamma$ -RPTP $\gamma$ ) in adult mouse brain: upregulation during neuroinflammation.**

Erika Lorenzetto<sup>1</sup>, Elisabetta Moratti<sup>2</sup>, Marzia Vezzalini<sup>2</sup>, Sheila Harroch<sup>3</sup>, Claudio Sorio<sup>2</sup> and Mario Buffelli<sup>1-4-5</sup>.

Author Affiliation

1. Dept. of Neurological, Neuropsychological, Morphological and Motor Sciences, Section of Physiology, University of Verona, Strada le Grazie 8, 37134 Verona-Italy.

2. Dept. of Pathology and Diagnostics, Section of General Pathology, University of Verona, Strada le Grazie 8, 37134 Verona-Italy

3. Dept. of Neuroscience, Institut Pasteur of Paris, 25-28 rue du Dr Roux, 75624 Paris, France.

4. Center for Biomedical Computing, University of Verona, Strada le Grazie 8, 37134 Verona-Italy

5. National Institute of Neuroscience-Italy

Corresponding authors: Prof. Mario Buffelli

Dept. of Neurological, Neuropsychological, Morphological and Motor Sciences, Section of Physiology, University of Verona, Strada le Grazie 8, 37134 Verona-Italy.

Tel. ++39045-8027268 Fax ++39045-8027279

Email: [mario.buffelli@univr.it](mailto:mario.buffelli@univr.it)

Dr. Erika Lorenzetto PhD

Dept. of Neurological, Neuropsychological, Morphological and Motor Sciences, Section of Physiology, University of Verona, Strada le Grazie 8, 37134 Verona-Italy.

Tel. ++39045-8027151 Fax ++39045-8027279

Email: [erika.lorenzetto@univr.it](mailto:erika.lorenzetto@univr.it)

### **Abstract**

The receptor protein tyrosine phosphatase  $\gamma$  (Ptp $\gamma$ -RPTP $\gamma$ ) is a receptor protein widely expressed in many tissues, including the central nervous system (CNS). Several RPTP $\gamma$  isoforms are expressed in the brain during development and in adulthood, but their distribution and role are unknown. In this study we investigated the distribution of some RPTP $\gamma$  isoforms in the adult brain by using antibodies against the epitopes localized in the C- and in the N-terminal domains of the full length isoform of RPTP $\gamma$ . We found a predominant and widespread neuronal positivity throughout the neocortex, hippocampus, striatum and in many nuclei of the brainstem and cerebellum. At least 2 distinct isoforms that can co-exist in various compartments in the same cell are detectable in different neuron types. Immunopositivity for epitopes located in both the N- and C-terminus domains were found in the neuropil of cortical and hippocampal neurons, whereas the N-terminal domain positivity was found in the soma, often without colocalization with its C-terminal counterpart. Among glial cells, some protoplasmic and perivascular astrocytes and the cerebellar Bergmann glia, express RPTP $\gamma$ . The astrocytic expression of RPTP $\gamma$  and putative processing isoforms of 120 and 80 kDa increases during neuroinflammation, in particular 24h after

LPS treatment. Activated astrocytes were found to be strongly positive for RPTP $\gamma$  also in a mice model of Alzheimer's disease. Our results confirm previous findings and enrich the current knowledge of RPTP $\gamma$  distribution in the CNS, highlighting a role of RPTP $\gamma$  during neuroinflammation processes.

Key words (4-6): RPTP $\gamma$ , neuroinflammation, LPS, RPTP $\zeta$ , reactive astrocytes and Alzheimer's disease.

## Introduction

It is now well established that in the brain receptor-subtype protein kinases and phosphatases are key regulators of signaling mechanisms underlying synaptic network orchestration (Dabrowski and Umemori 2011) and neuron-glia interactions (Faissner et al. 2006). While protein tyrosine kinases have been extensively studied so far, the role and the functions of receptor protein tyrosine phosphatases (RPTPs) are less known (for a review see Tonks 2006). RPTPs are classified into distinct groups, on the basis of their structure (Johnson and Van Vactor 2003). The Receptor Protein Tyrosine Phosphatase  $\gamma$  (RPTP $\gamma$ ) is a member of the V subgroup of Receptor PTPs together with its highly homologous PTP zeta (RPTP $\zeta$ ) (Barnea et al. 1993; Nishiwaki et al. 1998). The structure of these proteins includes a carbonic anhydrase-like domain and a fibronectin domain that together with a spacer region form the extracellular N-terminal portion. The intracellular C-terminal portion presents 2 tyrosine phosphatase domains, one of which lacks the catalytic activity (Barnea et al. 1993; Lamprianou and Harroch 2006). RPTP $\gamma$  is expressed in developing and adult vertebrates in many tissues, and its expression may change in pathological conditions (Vezzalini et al. 2007). RPTP $\gamma$  is present at high levels in the nervous system, but its role is currently unknown, although some ligands and a role in mental disorders have been proposed (Bouyain and Watking 2010; Hamshere et al. 2009; Zhang et al. 2012). Despite its high expression level in the brain, knockout (KO) mice develop normally and present only mild behavioral abnormalities (Lamprianou et al. 2006). RPTP $\gamma$  was not normally found in cortical astrocytes (Lamprianou et al. 2006), however its transcription can be induced by IL1 and TNF $\alpha$  in human astrogloma cell lines *in vitro* (Schumann et al. 1998).

Despite being mainly a neuronal protein, a thorough analysis of RPTP $\gamma$  distribution in the adult brain has been described using a knock-in mice where the promotor of RPTP $\gamma$  drive LacZ expression (Lamprianou et al. 2006). However this analysis did not allow the possibility to distinguish between the various isoforms of RPTP $\gamma$ . Importantly, at least 4 distinct RPTP $\gamma$  isoforms exist, including a truncated soluble PTP (sPTP $\gamma$ ), that lacks the intracellular catalytic C-terminal domains and it is thus devoid of the phosphatase activity (Shintani et al. 1997). One of the

limitations in studying different RPTP $\gamma$  isoforms is the scarceness of antibodies against different specific epitopes, especially toward the extracellular N-terminal region.

In this study we used different antibodies against C- and N-terminal epitopes, the last ones developed in our laboratory, in order to investigate the distribution of the intra- and of the extracellular domains of RPTP $\gamma$ , with the aim of evaluating whether specific isoforms (Sorio et al. 1995; Mafficini et al. 2007; Vezzalini et al. 2007) could be detectable in tissues. Moreover we investigated the consequence of neuroinflammation on its expression.

We found RPTP $\gamma$  expression in the neuropil of cortical neurons and in cerebellar Bergmann radial glia, whereas a truncated form lacking the C-terminal domain was present in the soma of cortical and hippocampal neurons, in Purkinje cells and interneurons of the cerebellar cortex. We also found that astrocytes upregulated both the full length and the truncated RPTP $\gamma$  isoform during neuroinflammation.

Overall our study highlights a role for RPTP $\gamma$  during astrocyte activation *in vivo* and highlight for the first time in situ a differential distribution of the C- and N-terminal portions, suggesting a complex post-translational regulation of RPTP $\gamma$  in the adult nervous system.

## **Materials and Methods**

### *Animals*

Mice were maintained under standard environmental conditions (temperature, humidity, 12 h/12 h light/dark cycle, with water and food *ad libitum*) under veterinarian assistance. Animals handling and surgery were performed following a protocol which received approval by the Animal Care and Use Committee of the University of Verona (CIRSAL), and authorization by the Italian Ministry of Health, in strict adherence to the European Communities Council (86/609/EEC) directives, minimizing the number of animals used and avoiding their suffering.

We used adult C57/BL6J mice purchased from Harlan. 5 months old 5XFAD mice were purchased from the Jackson Laboratory (Bar Harbor, Maine). Adult RPTP $\gamma$  deficient mice (129SveV) were generously given by Dr. S Harroch from the Institut Pasteur of Paris, France.

### *Immunofluorescence.*

Under deep anesthesia (tribromoethanol, intraperitoneal dose of 0,5 g/kg body weight) mice were transcardially perfused with paraformaldehyde 4% in saline buffer. The brain was excised, postfixed and cryoprotected before freezing. Brain slices (35 $\mu$ m thick) were obtained and stained with antibodies. Some mice were intraperitoneal (ip) injected with 500 $\mu$ g/kg of LPS (Life Technologies) and sacrificed 24h post injection.

Free floating cryosections were stained with different combinations of antibodies. Sections were permeabilized with the following solution: 2% Bovine Serum Albumin and 0,3% Triton X-100 in PBS, pH 7.4 for 30 minutes. Then sections were incubated overnight at 4°C with primary antibodies followed by the proper secondary Alexa Fluor-conjugated antibodies (1:1000, Life Technologies) for 1h at RT. Nuclei were stained with DAPI (Sigma). After mounting with an anti-fading solution, slices were studied by fluorescence microscopy (DM6000B, Leica Microsystem) and confocal microscopy (TCS-SP5, Leica Microsystem).

### *Antibodies*

The specificity of antibodies against N-terminus domain of Ptp<sup>prg</sup>-RPTP $\gamma$ : chicken anti-RPTP $\gamma$  (ch-RPTP $\gamma$ ) and rabbit anti-RPTP $\gamma$  (rb-RPTP $\gamma$ -P4) used in this study were previously described in detail (Sorio et al. 1995; Mafficini et al. 2007; Vezzalini et al. 2007, Della Peruta et al., 2010 Cancer Research). We also used anti-RPTP $\gamma$  C-terminus domain developed in goat (goat-RPTP $\gamma$  1:20 Santa Cruz) and anti-PTP $\zeta$ , (mouse IgG1, 1:250, BD Bioscience). The features of anti-RPTP $\gamma$  antibodies, together with the epitope localizations are given in Table 1.

Neuronal and glial markers used were: anti-MAP2 (mouse IgG1, 1:1000, Sigma-Aldrich), anti-NeuN (mouse IgG1, 1:200, Chemicon), anti- $\beta$ III-tubulin (Rabbit, 1:1000, Sigma-Aldrich), anti-Amyloid  $\beta$  clone 4G8 (IgG2b, 1:200, Covance), anti-Calbindin (IgG1, 1:500, Swant), anti-GFAP (IgG1, 1:500, Chemicon), anti-S100 (Rabbit, 1:400, Dako) and anti-CD11b (rat, 1:1000, Serotec).

### *Tissue lysate*

C57 mice were sacrificed by terminal anesthesia 24h after LPS or saline ip injection. After a transcardial perfusion with PBS/Heparin in order to discard the blood, brain cortices were quickly removed, frozen in liquid nitrogen vapor and stored at -80°C. Brain cortices were cut by cryostat and 30  $\mu$ m sections were homogenized in lysis buffer (LB) containing 50 mM Tris (pH 7.4), 1% Triton X-100, 150 mM NaCl, 200  $\mu$ M NaVO<sub>4</sub>, 1 mM EDTA, 1 mM DTT, 1 mM NaF and Complete EDTA-free Protease Inhibitor Cocktail Tablets (Roche, Germany), incubated for 20 min in a rotating wheel at 4°C and then centrifuged for 15 min at 4 °C at 15000  $\times$ g in a Biofuge Pico (DJB Labcare Ltd. UK). All the lysis procedures were carried out at 4°C.

### *Western Blot*

After protein quantification by Bradford assay, equal amounts of protein were resuspended in sample buffer (SB: 40 mM Tris-HCl pH 6.8, 183 mM  $\beta$ -mercaptoethanol, 1% SDS, 5% glycerol) and denatured at 95°C for 10 minutes. Lysates were resolved on 7,5 % SDS-PAGE and electroblotted onto polyvinylidene difluoride membrane (Millipore Corp., Bedford, MA). The

membrane was blocked with 5% BSA in TBS containing 0.05 % Tween-20 (TBST) for anti-GFAP (1:1000), and 5% skimmed milk for rb-RPTP $\gamma$ -P4 (1 $\mu$ g/ml) in 1% BSA TBST buffer overnight. After washes in TBST, the membrane was incubated with rabbit anti-goat-HRP (Sigma-Aldrich) or goat anti-mouse-HRP (GE Healthcare, Little Chalfont, UK) for 1 h. After washing with TBST, the signal was detected with the enhanced chemiluminescence kit (Millipore Corp., Bedford, MA) using an ImageQuant LAS 4000 (GE healthcare) imager. Band intensity was detected by Quantity One software (Biorad) and normalized to Ponceau Red staining.

## Results

### *1- RPTP $\gamma$ is a neuronal protein of widespread distribution in the adult mouse brain.*

In order to investigate the expression and distribution of RPTP $\gamma$  and related isoforms in the adult mouse brain, we stained brain sections with antibodies against either the extracellular N-terminal domain or the intracellular C-terminal portion. To detect the extracellular N-terminal domain we used antibodies made in chicken and developed in our laboratory (Vezzalini et al. 2007). Moreover, we used neuronal and glial markers to identify the different cell type. As shown in figure 1, we found that RPTP $\gamma$  was widely distributed throughout the brain, with immunopositivity in many neurons of the cerebral cortex and in the hippocampus. Its distribution was mainly neuronal, as demonstrated by  $\beta$ III-tubulin colocalization (Fig. 1 a-c). Astrocyte positivity was dependent on cell size and on the degree of Glial Fibrillary Acidic Protein (GFAP) expression: small astrocytes with thin GFAP-positive processes were negative to RPTP $\gamma$  (Fig. 1 j-l), whereas bigger astrocytes, such as those of the hippocampus (Fig. 1 d-f and m) or perivascular astrocytes (Fig. 1 g-i), with thick GFAP-positive processes were generally positive to RPTP $\gamma$ . Microglial cells were negative (Fig. 1 n-o).

In the cerebellum (Fig. 2), RPTP $\gamma$  positivity was found in the molecular layer, in Purkinje cells (soma and main dendrites but not in spiny branchlets) and interneurons as demonstrated by colocalization with  $\beta$ III-tubulin. Colocalization with the radial glial markers S100 and GFAP in the cerebellar cortex revealed a RPTP $\gamma$  positivity of Bergmann glial cells, the radial glia of the cerebellum. Almost all deep cerebellar nuclei were also strongly positive (not shown).

Using the fluorescence microscope we performed an atlas-based analysis of some coronal sections at different distances from the bregma, and we found that RPTP $\gamma$  was widely expressed in many structures throughout the brain. Results are summarized in Table 2. RPTP $\gamma$  immunoreactivity was present in different layers of the cerebral cortex, in the striatum, in many nuclei of the thalamus and of the brainstem, and it was generally a neuronal protein in the normal

adult mouse brain. Many elements of the white matter were negative, except for some big astrocytes. The wide distribution of RPTP $\gamma$  suggests that it may have a role in the building or maintenance of synaptic circuitry in the brain.

Differential labeling and confocal analysis of the C- and N-terminal domain epitopes show that the two portions of the phosphatase colocalize in the neuropil, but not in the soma of neurons, in which the N-terminal epitope positivity was mainly found (Fig. 3). Interestingly, in the cerebellum the two portions colocalize in Bergmann glial cells, thus indicating the presence of a full length RPTP $\gamma$  isoform. The N-terminal positivity was found alone in Purkinje cells and cerebellar interneurons, indicating the presence of truncated forms.

These data shows that distinct isoforms of RPTP $\gamma$  are present in different types of neurons/glial cells of the brain in physiological conditions.

We also performed a staining on a few slices of one heterozygous and one RPTP $\gamma$  KO mouse (Lamprianou et al. 2006). Despite some residual staining remained, we observed a strong reduction of the RPTP $\gamma$  positivity as compared to the heterozygous control (see supplementary figure).

### *2- RPTP $\gamma$ and RPTP $\zeta$ , expressions are distinct*

RPTP $\gamma$  and RPTP $\zeta$ , are members of the same family of tyrosine phosphatases and are highly homologous. To assess the specificity of our antibodies against RPTP $\gamma$ , we stained sections simultaneously for RPTP $\gamma$  and RPTP $\zeta$ , which resulted in a distinct staining pattern. Both proteins were neuronal, but RPTP $\zeta$  was observed as a spotted labeling along the neuropil both in the cortex and in the hippocampus (Fig. 4). Indeed the antibody anti- RPTP $\zeta$  recognizes the intracellular C-terminal phosphatase domain and therefore is able to detect 2 out of 3 RPTP $\zeta$  isoforms. A strong neuronal post-synaptic signal was previously reported by using this antibody together with a lack of positivity in cortical and hippocampal astrocytic processes (Hayashi et al. 2005). Thus it is not surprising that in our sections hippocampal astrocytes were negative for RPTP $\zeta$  (Fig. 4 i). In the cerebellum RPTP $\zeta$  was found only in Purkinje cell dendrites, but not in radial glia (Fig. 4 j-l). Our data show that the staining for RPTP $\zeta$ , and RPTP $\gamma$  in neurons were distinct and only partially overlapping, thus supporting the specificity of our antibodies against RPTP $\gamma$  and suggesting that the two proteins can be expected to have different and specific functions in neurons, even if they are highly homologous.

### *3- RPTP $\gamma$ distribution in inflammatory states: LPS and AD*

The expression of RPTP $\gamma$  in protoplasmic astrocytes with thick GFAP-positive branches under physiological conditions prompted us to investigate whether its expression could increase in brain during inflammation. Thus, we performed the staining of brain sections in mice sacrificed 24 h after LPS ip injection, a treatment that is known to cause a general brain inflammation and glial cell activation within 24 h from injection (Kwon et al. 2010). We found that activated GFAP-positive cortical astrocytes were strongly positive for RPTP $\gamma$ , while the protein distribution in neurons did not change significantly (Fig. 5 a to d). In order to quantify this phenomenon, we performed western blotting experiments on cerebral cortices of adult mice with or without LPS injections. As shown in Fig. 5 e, the increase of GFAP reflects the increase of activation state of astrocytes 24h after LPS treatment. We also performed western blotting using an anti-RPTP $\gamma$  antibody made in rabbit (Rb-RPTP $\gamma$ -P4) (Sorio et al. 1995), that revealed an increase, upon LPS treatment, of all the 3 isoforms detected: the full length RPTP $\gamma$  (180kDa band) and two truncated isoforms at 120 and 80kDa bearing the extracellular N-terminal portion that is recognized by the above mentioned antibody (Fig. 5 e). Interestingly, the densitometry revealed that after LPS the 120 kDa band, increased much more than the others (180 kDa) ( $p < 0,01$  by t-test). Moreover the normalized expression level of the isoforms remained linearly correlated among the 3 individual mice, with a  $r^2$  from of 0.67 to 0.77 (Fig 5 g to i), suggesting that the smaller isoforms might derive from proteolytic cleavage of the longers. As gel loading control the Ponceau staining is also shown.

We further confirmed that activated astrocytes express high levels of RPTP $\gamma$  in another model of brain inflammation: the 5XFAD mouse, one of the murine models of Alzheimer's disease (Oakley et al. 2006). We stained cerebral sections of a 6 months old mouse in order to detect amyloid plaques in the cerebral cortex by using the 4G8 antibody. This antibody labels amyloid  $\beta$  and its precursors such as the neuronal Amyloid Precursor Protein (APP), which are ubiquitously expressed in neurons. For this reason many neurons are positive for 4G8 staining (Fig. 6). In tissue sections the amyloid plaques are clearly recognizable by their morphology. The strong activation of astrocytes and microglia around the amyloid plaques is visualized by the cell morphology (astrocytes here are bigger and present thick processes) and the elevation of the specific markers GFAP and Cd11b. Also, in this model of neuroinflammation, neurons and astrocytes were strongly positive for RPTP $\gamma$ . On the contrary, both activated microglial cells and amyloid plaques were negative.

All together these data suggest that RPTP $\gamma$  is generally upregulated during neuroinflammation *in vivo* and might play a role in astrocyte activation.

## Discussion

In this study we investigated the distribution of RPTP $\gamma$  and related isoforms in the nervous system by using, for the first time in the literature, simultaneously antibodies against C- and N-terminus epitopes of the protein. These antibodies are able to distinguish between the full length (colocalization of C- and N- terminus) and the truncated isoforms lacking C-terminus domain (only N-terminus positivity) of the phosphatase. In line with previous studies (Lamprianou et al. 2006), we found a predominant and widespread neuronal RPTP $\gamma$  immunopositivity throughout the brain. Using the C- and N-terminus antibodies, we further analyzed the expression of RPTP $\gamma$ : both N- and C-terminus were found in the neuropil of cortical and hippocampal neurons demonstrating a RPTP $\gamma$  full length expression. The positivity for the N-terminal domain was found also in the soma, often without its C-terminal counterpart showing an expression of a shorter isoform in the soma. Thus, at least two isoforms of RPTP $\gamma$  are present in the adult normal murine brain and are differentially distributed not only in different types of neurons, but also in different compartments of the same cell. Clarifying whether the truncated N-terminal isoforms are produced by alternative splicing or by proteolytic cleavage starting from the full-length protein, will be object of further studies. Indeed a proteolytic cleavage *in vivo* have been already hypothesized, but not yet demonstrated, studying the changes in RPTP $\gamma$  expression during mouse development in the superior colliculus: here three different isoforms were detected at different time points from E13 to P20 (Reinhard et al. 2009).

It was reported that RPTP $\gamma$  KO mice did not show any obvious phenotype, displaying only minor behavioral changes, in spite of the expression during development and in the adult brain in pyramidal and sensory neurons (Lamprianou et al. 2006; Zhang et al., 2012). Indeed RPTP $\gamma$  is highly homologous to RPTP $\zeta$ , and both are expressed in neurons (Shintani et al. 1998; Tanaka et al. 2003; Hayashi et al. 2005), suggesting that potentially they might have overlapping activities at the occurrence and RPTP $\zeta$ , could compensate the loss of RPTP $\gamma$ . We stained our sections simultaneously for RPTP $\gamma$  and for RPTP $\zeta$ , and found only partial overlapping signals in neurons and, an overall different staining pattern. Beside supporting the specificity of the antibodies against the N-terminal portion of RPTP $\gamma$  these results suggest that PTPs other than RPTP $\zeta$  might compensate for RPTP $\gamma$  loss during the embryonal development of KO mice.

This report supports the previous studies on the pattern of expression of RPTP $\gamma$  and RPTP $\zeta$ . Despite it is reported that RPTP $\zeta$  is strongly expressed in glial cells (oligodendrocytes and astrocytes) we found a spotted-like positivity in cortical and hippocampal neurons, in line with previous studies that used the same antibodies (Hayashi et al. 2005), while RPTP $\gamma$  had a very strong expression in neurons (Lamprianou et al, 2006). We show that most perivascular astrocytes

do not express RPTP $\gamma$  in normal adult mouse brain, and that in some sublocalisation of neurons both RPTP $\zeta$  and RPTP $\gamma$  can be detected.

The RPTP $\gamma$  role and function in the adult CNS is unknown and largely unexplored, as well as are its ligands. RPTP $\gamma$  could putatively bind to contactins-3, -4 and -5 that are widely distributed in the adult brain, but the meaning of this interaction is unclear (Bouyain and Watkins 2010; Lamprianou et al. 2011; Hendriks et al. 2013). Some recent data support a function of RPTP $\gamma$  in depression (Zhang et al. 2012) and bipolar disorders (Hamshere et al. 2009). This is in line with its potential interaction with the CNTNs and CNTNs signaling pathway, which are genes mutated in mental disorders (Cottrel et al. 2011).

In chick spinal cord RPTP $\gamma$  plays a role in spinal cord neurogenesis during embryonic development, where it appears to influence the Wnt/ $\beta$  catenin signaling and neuronal survival (Hashemi et al. 2011). Moreover RPTP $\gamma$  inhibits the NGF-mediated neurite outgrowth in PC12 cells (Shintani et al. 2001). Our study is the first that describes the distribution of different RPTP $\gamma$  isoforms in the brain, and it completes and enriches the current knowledge about the distribution of RPTP $\gamma$  and could help in developing new hypotheses about its role and molecular mechanisms in neurons of the adult brain.

Another major finding of our study is that, despite not being expressed in small astrocytes, RPTP $\gamma$  is up-regulated in these same cells following intraperitoneal injection of LPS and in the 5XFAD murine model of Alzheimer's disease, two well characterized *in vivo* models of brain inflammation. These data suggest, for the first time *in vivo*, that RPTP $\gamma$  can be involved in the process of astrocyte activation. It is already known that, after Interleukin 1  $\beta$  (IL1  $\beta$ ) and Tumor Necrosis Factor alpha (TNF $\alpha$ ) treatment *in vitro*, RPTP $\gamma$  mRNA is upregulated by human astrocytoma cells (Schumann et al. 1998). Indeed after LPS ip treatment both IL1  $\beta$  and TNF $\alpha$  mRNA are upregulated in mouse brain within 90min, and the astrocyte activation reaches its maximum at 24h post injection (Kwon et al. 2010). In this study we showed that 24h after LPS injection the increase in GFAP level is accompanied by the increase in RPTP $\gamma$  protein level in brain astrocytes. This is the first time that this increase is demonstrated *in vivo* on different isoforms of RPTP $\gamma$ . Indeed, we observed a marked increase of the 120 kDa truncated RPTP $\gamma$  isoform by WB after LPS treatment. Since all isoforms present a reciprocal linear correlation, it might be possible that the truncated isoforms are produced in part by cleavage starting from the longer ones. Interestingly following LPS treatment, activated microglia and astrocytes are known to produce many different matrix metalloproteases like MMP-3 and MMP-9 (Gottschall and Deb 1996; Lee et al. 2003). Cytokines like IL1  $\beta$  and TNF $\alpha$  are potent stimulant of MMPs production by activated glia *in vitro* (Gottschall and Yu 1995; Crocker et al. 2006; for a review see Candelario-Jalil et al. 2009). The possible role of matrix metalloproteases in the cleavage of

RPTP $\gamma$  during neuroinflammation will be object of further studies. Indeed we cannot exclude that short and long isoforms are produced by alternative splicing, as happens for RPTP $\zeta$ , that is highly homologous to RPTP $\gamma$ .

As concern the RPTP $\zeta$  signal, we found a punctuate staining pattern in neurons, in line with previous studies where this protein was found to be localized post-synaptically and not in astrocytes when the same antibody was used (Hayashi et al. 2005; Kawachi et al. 1999). It has been reported for long time that RPTP $\zeta$  is expressed in astrocytes (Canoll et al. 1996; Sakurai et al. 1996;). Among the three splicing variants, its soluble isoform phosphacan lacking the intracellular domain is released during inflammation or lesion (Faissner et al. 2006). A possible explanation for this lack of positivity in astrocytes might be that mature astrocytes preferentially express the phosphacan isoform (Canoll 1996 et al.; Sakurai 1996 et al.), which is not detected by this antibody.

More recent studies suggest that the neuronal RPTP $\zeta$  isoforms might play a critical role in the reactive synaptogenesis occurring after injury (Harris et al., 2011). Indeed the last decade of research on Phosphacan/RPTP $\zeta$  isoforms reveals a high degree of complexity in the regulation and roles of this particular phosphatase in both physiological and pathological conditions (Lamprianou et al. 2011; Hendriks et al. 2013).

In this study, we show an increased expression of the RPTP $\gamma$  isoform lacking the D2 domain upon inflammation. RPTP $\gamma$  inhibits NGF signaling and therefore TRK dependent axon growth (Shintani 2001). Using different signaling pathways, RPTP $\zeta$  and RPTP $\gamma$  could generate similar biological function such as modulating neurite outgrowth during inflammation. The increased expression of the RPTP $\gamma$  isoform lacking a C-terminal portion, likely including the D2 domain, is of interest. Indeed structural biology of PTPs proposed that these proteins homodimerize inducing inhibition of the phosphatase activity by changing the relative position of the D1 and D2 domains (Tremblay 2009; Barr et al. 2009). Thus, an isoform lacking the D2 domain could not be inhibited by this mechanism and could strengthen its efficacy to dephosphorylate the NGF/TRK signaling or other still unidentified pathways.

In this line both phosphatase RPTP $\gamma$  and RPTP $\zeta$  should increase in astrocytes when inflammation occurs. Indeed, as one of the main components of Chondroitin Sulfate Proteoglycans (CSPGs), phosphacan is expressed at high level by reactive astrocytes upon injury, and prevent axon growth by direct binding to the surface of the growth cone and by interacting with L1/NgCAM/laminin substrates (for a review see Sandvig et al., 2004). RPTP $\gamma$  is also expressed upon cytokines treatment and inflammation. If both phosphatases have only partial overlap of expression, they might address similar biological function.

Overall, our study enriches the current knowledge about the role of RPTP $\gamma$  in astrocyte activation *in vivo* and the differential distribution of RPTP $\gamma$  isoforms could help in making new hypothesis about the mechanism of action/role of the phosphatase in neuronal physiological functions.

#### ACKNOWLEDGEMENTS

This work was supported by University of Verona and Fondazione Cariverona-project Verona Nanomedicine Initiative. Development and characterization of antibodies were supported by AIRC IG 4667 and Consorzio per gli Studi Universitari, Verona.

Conflict of Interest: The authors declare no competing financial interests.

#### Figure Legends

##### **Fig. 1 RPTP $\gamma$ is expressed in neurons and in some astrocytes in the adult brain.**

Examples of immunostaining showing the RPTP $\gamma$  positivity of neurons (a-c), astrocytes and microglia (d-o). Colocalization of RPTP $\gamma$  (green) and  $\beta$ III-tubulin (blue) shows the neuronal expression of RPTP $\gamma$  in the cerebral cortex (a-c). Astrocytes are labeled by GFAP (red). In a and c astrocytes surrounding a blood vessel are also shown (red).

A representative image of the dentate gyrus shows the mild colocalization of RPTP $\gamma$  and GFAP, indicating the positivity of some astrocytes in the hippocampus (d-f) as well as those surrounding some blood vessels (g-i). Small astrocytes (j-l) are negative for RPTP $\gamma$ , whereas a mild positivity was found only in some big astrocytes (GFAP red in m) but not in the resting microglia labeled by CD11b (red in n and o). In some images the nuclear DAPI staining is also shown. Scale bars 50 $\mu$ m in a to f, 20 $\mu$ m in g to o.

##### **Fig. 2 RPTP $\gamma$ is expressed in neurons of the cerebellar molecular layer and in cerebellar radial glia.**

Immunostaining showing the RPTP $\gamma$  expression in the cerebellar cortex of adult mouse brain. (a-d) Colocalization of RPTP $\gamma$  (green) and  $\beta$ III-tubulin (red) shows positivity for interneurons of the molecular layer, as well as Purkinje cell main dendrite. e-h. Colocalization of RPTP $\gamma$  and GFAP (red) shows positivity for Bergmann radial glia. g and h are enlargements of the boxed region in f. (i-l) Colocalization of RPTP $\gamma$  and the Bergmann glia specific marker S100 (red) confirms the expression of RPTP $\gamma$  in these cells. k is an enlargement of the boxed region in j. In some images nuclei counterstaining by DAPI (blue) is also shown. ML: molecular layer; PL: Purkinje cell layer; GCL: granule cell layer. Scale bars 20 $\mu$ m in g, h, k, l, 40 $\mu$ m in all the other images.

**Fig. 3 RPTP $\gamma$  C- and N-terminal epitopes are differently localized within brain cells.**

Immunostaining of brain sections by using different antibodies against either the N- (anti-RPTP $\gamma$  chicken isotype, green) or the C-terminal (red) portion of RPTP $\gamma$  allows to distinguish between the full length protein (colocalization) and a truncated isoform lacking the C-terminus epitope (green only). (a-b) cerebral cortex shows that the N- and C-terminus colocalizes in the apical dendrite and in some neurons, but the soma mainly presents the N-terminus positivity alone. (c-d) enlargements of the boxed region in a. (e-h) shows that resting astrocytes (GFAP, blue) are negative for both epitopes. (i-l) Cerebellar cortex displays C- and N- terminus colocalization only in Bergamnn radial glia, whereas the N-terminal epitope is present alone in Purkinje cells and colocalizes with Calbindin (blue). ML: molecular layer; PL: Purkinje cell layer. Scale bars 30 $\mu$ m in a, b, i, j, k, l; 15 $\mu$ m in c, d, e, f, g, h.

**Fig. 4 Comparison of the distribution of RPTP $\zeta$  and RPTP $\gamma$  receptors.**

Immunostaining of brain sections by using anti-RPTP $\gamma$  (antibody made in chicken) and anti-RPTP $\zeta$ , a protein that is highly homologous with RPTP $\gamma$ . a-f Cerebral cortex, where colocalization of RPTP $\gamma$  (green) and RPTP $\zeta$ , (red) occurs in the neuropil ( $\beta$ III-tubulin, blue). f is an enlargement of the boxed region in d and shows the spotted staining pattern of RPTP $\zeta$ . g-i In the hippocampus both proteins are neuronal. The boxed region enlarged in i shows astrocytes that are negative for RPTP $\zeta$  (arrows). j-l In the cerebellar cortex RPTP $\zeta$  was found in Purkinje cell primary dendrites where it partially colocalizes with RPTP $\gamma$ .

The different localizations and staining patterns of RPTP $\zeta$ , and RPTP $\gamma$  further support the specificity of our N-terminal antibodies against RPTP $\gamma$  N-terminal domain. ML: molecular layer; PL: Purkinje cell layer. Scale bars 30 $\mu$ m.

**Fig. 5 RPTP $\gamma$  expression increases in astrocytes after LPS injection.**

RPTP $\gamma$  expression in mouse brain cortex 24h after LPS i.p. injection was assessed by immunostaining and WB. (a-d) Immunostaining showing a strong positivity for RPTP $\gamma$  (green) in activated astrocytes (GFAP, red; colocalization yellow). The boxed region of a is enlarged in b, c and d, in order to highlight activated astrocytes surrounding a blood vessel. Scale bars 30 $\mu$ m. (e) WB of brain cortex lysates of 3 normal (-) and 3 LPS (+) treated mice. Band intensity of RPTP $\gamma$  was detected by an antibody made in rabbit (rb-RPTP $\gamma$ -P4). Bands at 180kDa show the full length protein isoform, whereas at 120 and 80 kDa we found two truncated isoforms. GFAP increase confirms the astrocyte activation after LPS injection. Ponceau staining was used for normalization of the loaded protein. The densitometry plot (f) shows the normalized band intensity relative to 120 and 180kDa isoforms with or without LPS treatment. All isoforms increased after LPS

treatment, especially the truncated 120kDa RPTP $\gamma$ .  $p < 0,01$  by t-test. (g-i) Plots showing the strong linear correlation between the normalized intensities of the 3 RPTP $\gamma$  isoforms showed in e, suggesting their origin from a common precursor.

**Fig. 6 RPTP $\gamma$  is expressed in cortical activated astrocytes in the murine model of Alzheimer's disease.**

Expression of RPTP $\gamma$  (green) was assessed in brain cortex of a 6 month old 5xFAD mouse brain by immunostaining. Staining for amyloid  $\beta$  peptide (4G8, red) shows neuronal APP and amyloid plaques (red). (a-b) RPTP $\gamma$  (green) is neuronal, but a strong positivity was found also in astrocytes (GFAP, blue in a, red in b, false color). (c) shows the colocalization of RPTP $\gamma$  (green) and 4G8 (red) in neurons but not in amyloid plaques. (d-f) Activated microglia (CD11b, red) surrounding amyloid plaques is negative for RPTP $\gamma$ . (f) represents an enlargement of the boxed region in d. (g-i) Neuronal expression of RPTP $\gamma$  in AD mice assessed by colocalization with MAP2 (blue in g and red in h, false color). Scale bars 40  $\mu$ m in a-e, 20  $\mu$ m in f-i.

**Supplementary figure**

As an additional test for antibody specificity we stained some slides from one heterozygous and one RPTP $\gamma$  KO mouse using the two antibodies against the N- (ch-RPTP $\gamma$ , green) and the C-terminus (goat-RPTP $\gamma$ , red) epitopes of the phosphatase. Cerebral cortex (A-F and J-O) and hippocampus (G-I and P-R) showed a strong decrease of RPTP $\gamma$  signal in the KO (J to R) in comparison to the heterozygous (A to I). A residual staining was still present in some regions, in particular in the granular layer of the hippocampus, a region known to be prone to aspecific staining. Scale bars 50 $\mu$ m.

**Table 1**

Schematic representation of the antibodies used against RPTP $\gamma$ . Epitopes: amino acid number of epitopes, validated application: IP= immuno-precipitation, WB= western blot, IHC= immuno histo chemistry, Flow= flow cytometry, IF= immuno fluorescence. The RPTP $\gamma$  structure scheme displays where the epitopes are localized within the predicted protein sequence of the 4 different isoforms. CA: Carbonic anhydrase-like; FNIII: Fibronectin type III-like domain; TM: transmembrane portion; D1: active phosphatase domain and D2: inactive phosphatase domain.

**Table 2**

Distribution of RPTP $\gamma$  positivity in mouse brain coronal sections, assessed by immunostaining and fluorescence microscopy.

## References

- Barnea G, Silvennoinen O, Shaanan B, Honegger AM, Canoll PD, D'Eustachio P, Morse B, Levy JB, Laforgia S, Huebner K, et al. (1993) Identification of a carbonic anhydrase-like domain in the extracellular region of RPTP gamma defines a new subfamily of receptor tyrosine phosphatases. *Mol Cell Biol* 13 (3):1497-1506
- Barr, A. J., Ugochukwu, E., Lee, W. H., King, O. N., Filippakopoulos, P., Alfano, I., et al. (2009). Large-scale structural analysis of the classical human protein tyrosine phosphatome. [Research Support, Non-U.S. Gov't]. *Cell*, 136(2), 352-363, doi:10.1016/j.cell.2008.11.038.
- Bouyain S, Watkins DJ (2010) The protein tyrosine phosphatases PTPRZ and PTPRG bind to distinct members of the contactin family of neural recognition molecules. *Proc Natl Acad Sci U S A* 107 (6):2443-2448. doi:0911235107 [pii] 10.1073/pnas.0911235107
- Candelario-Jalil E, Yang Y, Rosenberg GA (2009) Diverse roles of matrix metalloproteinases and tissue inhibitors of metalloproteinases in neuroinflammation and cerebral ischemia. *Neuroscience* 158 (3):983-994. doi:S0306-4522(08)00895-6 [pii] 10.1016/j.neuroscience.2008.06.025
- Canoll, P. D., Petanceska, S., Schlessinger, J., & Musacchio, J. M. (1996). Three forms of RPTP-beta are differentially expressed during gliogenesis in the developing rat brain and during glial cell differentiation in culture. [Research Support, U.S. Gov't, P.H.S.]. *J Neurosci Res*, 44(3), 199-215, doi:10.1002/(SICI)1097-4547(19960501)44:3<199::AID-JNR1>3.0.CO;2-B.
- Cottrell, C. E., Bir, N., Varga, E., Alvarez, C. E., Bouyain, S., Zernzach, R., et al. (2011). Contactin 4 as an autism susceptibility locus. [Case Reports Research Support, N.I.H., Extramural Research Support, U.S. Gov't, Non-P.H.S.]. *Autism Res*, 4(3), 189-199, doi:10.1002/aur.184.
- Crocker SJ, Milner R, Pham-Mitchell N, Campbell IL (2006) Cell and agonist-specific regulation of genes for matrix metalloproteinases and their tissue inhibitors by primary glial cells. *J Neurochem* 98 (3):812-823. doi:JNC3927 [pii] 10.1111/j.1471-4159.2006.03927.x
- Dabrowski A, Umemori H (2011) Orchestrating the synaptic network by tyrosine phosphorylation signalling. *J Biochem* 149 (6):641-653. doi:mvr047 [pii] 10.1093/jb/mvr047

- Della Peruta M, Martinelli G, Moratti E, Pintani D, Vezzalini M, Mafficini A, Grafone T, Iacobucci I, Soverini S, Murineddu M, Vinante F, Tecchio C, Piras G, Gabbas A, Monne M, Sorio C (2010) Protein tyrosine phosphatase receptor type  $\{\gamma\}$  is a functional tumor suppressor gene specifically downregulated in chronic myeloid leukemia. *Cancer research* 70 (21):8896-8906. doi:10.1158/0008-5472.CAN-10-0258
- Faissner A, Heck N, Dobbertin A, Garwood J (2006) DSD-1-Proteoglycan/Phosphacan and receptor protein tyrosine phosphatase-beta isoforms during development and regeneration of neural tissues. *Adv Exp Med Biol* 557:25-53. doi:10.1007/0-387-30128-3\_3
- Gottschall PE, Deb S (1996) Regulation of matrix metalloproteinase expressions in astrocytes, microglia and neurons. *Neuroimmunomodulation* 3 (2-3):69-75
- Gottschall PE, Yu X (1995) Cytokines regulate gelatinase A and B (matrix metalloproteinase 2 and 9) activity in cultured rat astrocytes. *J Neurochem* 64 (4):1513-1520
- Hamshere, M. L., Green, E. K., Jones, I. R., Jones, L., Moskvina, V., Kirov, G., et al. (2009). Genetic utility of broadly defined bipolar schizoaffective disorder as a diagnostic concept. [Comparative Study Research Support, Non-U.S. Gov't]. *Br J Psychiatry*, 195(1), 23-29, doi:10.1192/bjp.bp.108.061424.
- Harris, J. L., Reeves, T. M., & Phillips, L. L. (2011). Phosphacan and receptor protein tyrosine phosphatase beta expression mediates deafferentation-induced synaptogenesis. [Research Support, N.I.H., Extramural]. *Hippocampus*, 21(1), 81-92, doi:10.1002/hipo.20725.
- Hashemi H, Hurley M, Gibson A, Panova V, Tchetchelnitski V, Barr A, Stoker AW (2011) Receptor tyrosine phosphatase PTPgamma is a regulator of spinal cord neurogenesis. *Mol Cell Neurosci* 46 (2):469-482. doi:S1044-7431(10)00263-0 [pii] 10.1016/j.mcn.2010.11.012
- Hayashi N, Oohira A, Miyata S (2005) Synaptic localization of receptor-type protein tyrosine phosphatase zeta/beta in the cerebral and hippocampal neurons of adult rats. *Brain Res* 1050 (1-2):163-169. doi:S0006-8993(05)00787-0 [pii] 10.1016/j.brainres.2005.05.047
- Hendriks, W. J., Elson, A., Harroch, S., Pulido, R., Stoker, A., & den Hertog, J. (2013). Protein tyrosine phosphatases in health and disease. *FEBS J*, 280(2), 708-730, doi:10.1111/febs.12000.
- Johnson KG, Van Vactor D (2003) Receptor protein tyrosine phosphatases in nervous system development. *Physiol Rev* 83 (1):1-24. doi:10.1152/physrev.00016.2002

- Kawachi, H., Tamura, H., Watakabe, I., Shintani, T., Maeda, N., & Noda, M. (1999). Protein tyrosine phosphatase zeta/RPTPbeta interacts with PSD-95/SAP90 family. [Research Support, Non-U.S. Gov't]. *Brain Res Mol Brain Res*, 72(1), 47-54.
- Kwon MS, Seo YJ, Choi SM, Won MH, Lee JK, Park SH, Jung JS, Sim YB, Suh HW (2010) The time-dependent effect of lipopolysaccharide on kainic acid-induced neuronal death in hippocampal CA3 region: possible involvement of cytokines via glucocorticoid. *Neuroscience* 165 (4):1333-1344. doi:S0306-4522(09)01971-X [pii]  
10.1016/j.neuroscience.2009.11.060
- Lamprianou S, Chatzopoulou E, Thomas JL, Bouyain S, Harroch S (2011) A complex between contactin-1 and the protein tyrosine phosphatase PTPRZ controls the development of oligodendrocyte precursor cells. *Proc Natl Acad Sci U S A* 108 (42):17498-17503. doi:1108774108 [pii]  
10.1073/pnas.1108774108
- Lamprianou S, Harroch S (2006) Receptor protein tyrosine phosphatase from stem cells to mature glial cells of the central nervous system. *J Mol Neurosci* 29 (3):241-255. doi:JMNM:29:3:241 [pii]  
10.1385/JMNM:29:3:241
- Lamprianou S, Vacaresse N, Suzuki Y, Meziane H, Buxbaum JD, Schlessinger J, Harroch S (2006) Receptor protein tyrosine phosphatase gamma is a marker for pyramidal cells and sensory neurons in the nervous system and is not necessary for normal development. *Mol Cell Biol* 26 (13):5106-5119. doi:26/13/5106 [pii]  
10.1128/MCB.00101-06
- Lee WJ, Shin CY, Yoo BK, Ryu JR, Choi EY, Cheong JH, Ryu JH, Ko KH (2003) Induction of matrix metalloproteinase-9 (MMP-9) in lipopolysaccharide-stimulated primary astrocytes is mediated by extracellular signal-regulated protein kinase 1/2 (Erk1/2). *Glia* 41 (1):15-24. doi:10.1002/glia.10131
- Mafficini A, Vezzalini M, Zamai L, Galeotti L, Bergamini G, Della Peruta M, Melotti P, Sorio C (2007) Protein Tyrosine Phosphatase Gamma (PTPgamma) is a Novel Leukocyte Marker Highly Expressed by CD34 Precursors. *Biomark Insights* 2:218-225
- Nishiwaki T, Maeda N, Noda M (1998) Characterization and developmental regulation of proteoglycan-type protein tyrosine phosphatase zeta/RPTPbeta isoforms. *J Biochem* 123 (3):458-467
- Oakley H, Cole SL, Logan S, Maus E, Shao P, Craft J, Guillozet-Bongaarts A, Ohno M, Disterhoft J, Van Eldik L, Berry R, Vassar R (2006) Intraneuronal beta-amyloid aggregates, neurodegeneration, and neuron loss in transgenic mice with five familial

- Alzheimer's disease mutations: potential factors in amyloid plaque formation. *J Neurosci* 26 (40):10129-10140. doi:26/40/10129 [pii]  
10.1523/JNEUROSCI.1202-06.2006
- Reinhard J, Horvat-Brocker A, Illes S, Zaremba A, Knyazev P, Ullrich A, Faissner A (2009) Protein tyrosine phosphatases expression during development of mouse superior colliculus. *Exp Brain Res* 199 (3-4):279-297. doi:10.1007/s00221-009-1963-6
- Romero-Calvo I, Ocon B, Martinez-Moya P, Suarez MD, Zarzuelo A, Martinez-Augustin O, de Medina FS (2010) Reversible Ponceau staining as a loading control alternative to actin in Western blots. *Anal Biochem* 401 (2):318-320. doi:S0003-2697(10)00135-1 [pii]  
10.1016/j.ab.2010.02.036
- Sakurai, T., Friedlander, D. R., & Grumet, M. (1996). Expression of polypeptide variants of receptor-type protein tyrosine phosphatase beta: the secreted form, phosphacan, increases dramatically during embryonic development and modulates glial cell behavior in vitro. [Research Support, Non-U.S. Gov't Research Support, U.S. Gov't, P.H.S.]. *J Neurosci Res*, 43(6), 694-706, doi:10.1002/(SICI)1097-4547(19960315)43:6<694::AID-JNR6>3.0.CO;2-9.
- Sandvig, A., Berry, M., Barrett, L. B., Butt, A., & Logan, A. (2004). Myelin-, reactive glia-, and scar-derived CNS axon growth inhibitors: expression, receptor signaling, and correlation with axon regeneration. [Review]. *Glia*, 46(3), 225-251, doi:10.1002/glia.10315.
- Schumann G, Fiebich BL, Menzel D, Hull M, Butcher R, Nielsen P, Bauer J (1998) Cytokine-induced transcription of protein-tyrosine-phosphatases in human astrocytoma cells. *Brain Res Mol Brain Res* 62 (1):56-64. doi:S0169328X9800237X [pii]
- Shintani T, Maeda N, Nishiwaki T, Noda M (1997) Characterization of rat receptor-like protein tyrosine phosphatase gamma isoforms. *Biochem Biophys Res Commun* 230 (2):419-425. doi:S0006-291X(96)95973-2 [pii]  
10.1006/bbrc.1996.5973
- Shintani T, Maeda N, Noda M (2001) Receptor-like protein tyrosine phosphatase gamma (RPTPgamma), but not PTPzeta/RPTPbeta, inhibits nerve-growth-factor-induced neurite outgrowth in PC12D cells. *Dev Neurosci* 23 (1):55-69. doi:48696 [pii]
- Shintani T, Watanabe E, Maeda N, Noda M (1998) Neurons as well as astrocytes express proteoglycan-type protein tyrosine phosphatase zeta/RPTPbeta: analysis of mice in which the PTPzeta/RPTPbeta gene was replaced with the LacZ gene. *Neurosci Lett* 247 (2-3):135-138

- Sorio C, Mendrola J, Lou Z, LaForgia S, Croce CM, Huebner K (1995) Characterization of the receptor protein tyrosine phosphatase gene product PTP gamma: binding and activation by triphosphorylated nucleosides. *Cancer Res* 55 (21):4855-4864
- Tanaka M, Maeda N, Noda M, Marunouchi T (2003) A chondroitin sulfate proteoglycan PTPzeta /RPTPbeta regulates the morphogenesis of Purkinje cell dendrites in the developing cerebellum. *J Neurosci* 23 (7):2804-2814. doi:23/7/2804 [pii]
- Tonks NK (2006) Protein tyrosine phosphatases: from genes, to function, to disease. *Nat Rev Mol Cell Biol* 7 (11):833-846. doi:nrm2039 [pii]  
10.1038/nrm2039
- Tremblay, M. L. (2009). The PTP family photo album. [Comment]. *Cell*, 136(2), 213-214, doi:10.1016/j.cell.2009.01.006.
- Vezzalini M, Mombello A, Menestrina F, Mafficini A, Della Peruta M, van Niekerk C, Barbareschi M, Scarpa A, Sorio C (2007) Expression of transmembrane protein tyrosine phosphatase gamma (PTPgamma) in normal and neoplastic human tissues. *Histopathology* 50 (5):615-628. doi:HIS2661 [pii]  
10.1111/j.1365-2559.2007.02661.x
- Zhang W, Savelieva K V, Tran D, Pogorelov V M, Cullinan E B, Backer K B, Platt K A, Hu S, Rajan I, Xu N, Lanthorn T H (2012) Characterization of PTPRG in knockdown and phosphatase-inactive mutant mice and substrate trapping analysis of PTPRG in mammalian cells. *Plos One* 7 (9) e45500. doi:10.1371/journal.pone.0045500

## **Distribution of different isoforms of Receptor Protein Tyrosine Phosphatase $\gamma$ (Ptp $\gamma$ -RPTP $\gamma$ ) in adult mouse brain: upregulation during neuroinflammation.**

Erika Lorenzetto<sup>1</sup>, Elisabetta Moratti<sup>2</sup>, Marzia Vezzalini<sup>2</sup>, Sheila Harroch<sup>3</sup>, Claudio Sorio<sup>2</sup> and Mario Buffelli<sup>1-4-5</sup>.

Author Affiliation

1. Dept. of Neurological, Neuropsychological, Morphological and Motor Sciences, Section of Physiology, University of Verona, Strada le Grazie 8, 37134 Verona-Italy.

2. Dept. of Pathology and Diagnostics, Section of General Pathology, University of Verona, Strada le Grazie 8, 37134 Verona-Italy

3. Dept. of Neuroscience, Institut Pasteur of Paris, 25-28 rue du Dr Roux, 75624 Paris, France.

4. Center for Biomedical Computing, University of Verona, Strada le Grazie 8, 37134 Verona-Italy

5. National Institute of Neuroscience-Italy

Corresponding authors: Prof. Mario Buffelli

Dept. of Neurological, Neuropsychological, Morphological and Motor Sciences, Section of Physiology, University of Verona, Strada le Grazie 8, 37134 Verona-Italy.

Tel. ++39045-8027268 Fax ++39045-8027279

Email: [mario.buffelli@univr.it](mailto:mario.buffelli@univr.it)

Dr. Erika Lorenzetto PhD

Dept. of Neurological, Neuropsychological, Morphological and Motor Sciences, Section of Physiology, University of Verona, Strada le Grazie 8, 37134 Verona-Italy.

Tel. ++39045-8027151 Fax ++39045-8027279

Email: [erika.lorenzetto@univr.it](mailto:erika.lorenzetto@univr.it)

### **Abstract**

The receptor protein tyrosine phosphatase  $\gamma$  (Ptp $\gamma$ -RPTP $\gamma$ ) is a receptor protein widely expressed in many tissues, including the central nervous system (CNS). Several RPTP $\gamma$  isoforms are expressed in the brain during development and in adulthood, but their distribution and role are unknown. In this study we investigated the distribution of some RPTP $\gamma$  isoforms in the adult brain by using antibodies against the epitopes localized in the C- and in the N-terminal domains of the full length isoform of RPTP $\gamma$ . We found a predominant and widespread neuronal positivity throughout the neocortex, hippocampus, striatum and in many nuclei of the brainstem and cerebellum. At least 2 distinct isoforms that can co-exist in various compartments in the same cell are detectable in different neuron types. Immunopositivity for epitopes located in both the N- and C-terminus domains were found in the neuropil of cortical and hippocampal neurons, whereas the N-terminal domain positivity was found in the soma, often without colocalization with its C-terminal counterpart. Among glial cells, some protoplasmic and perivascular astrocytes and the cerebellar Bergmann glia, express RPTP $\gamma$ . The astrocytic expression of RPTP $\gamma$  and putative processing isoforms of 120 and 80 kDa increases during neuroinflammation, in particular 24h after

LPS treatment. Activated astrocytes were found to be strongly positive for RPTP $\gamma$  also in a mice model of Alzheimer's disease. Our results confirm previous findings and enrich the current knowledge of RPTP $\gamma$  distribution in the CNS, highlighting a role of RPTP $\gamma$  during neuroinflammation processes.

Key words (4-6): RPTP $\gamma$ , neuroinflammation, LPS, RPTP $\zeta$ , reactive astrocytes and Alzheimer's disease.

## Introduction

It is now well established that in the brain receptor-subtype protein kinases and phosphatases are key regulators of signaling mechanisms underlying synaptic network orchestration (Dabrowski and Umemori 2011) and neuron-glia interactions (Faissner et al. 2006). While protein tyrosine kinases have been extensively studied so far, the role and the functions of receptor protein tyrosine phosphatases (RPTPs) are less known (for a review see Tonks 2006). RPTPs are classified into distinct groups, on the basis of their structure (Johnson and Van Vactor 2003). The Receptor Protein Tyrosine Phosphatase  $\gamma$  (RPTP $\gamma$ ) is a member of the V subgroup of Receptor PTPs together with its highly homologous PTP zeta (RPTP $\zeta$ ) (Barnea et al. 1993; Nishiwaki et al. 1998). The structure of these proteins includes a carbonic anhydrase-like domain and a fibronectin domain that together with a spacer region form the extracellular N-terminal portion. The intracellular C-terminal portion presents 2 tyrosine phosphatase domains, one of which lacks the catalytic activity (Barnea et al. 1993; Lamprianou and Harroch 2006). RPTP $\gamma$  is expressed in developing and adult vertebrates in many tissues, and its expression may change in pathological conditions (Vezzalini et al. 2007). RPTP $\gamma$  is present at high levels in the nervous system, but its role is currently unknown, although some ligands and a role in mental disorders have been proposed (Bouyain and Watking 2010; Hamshere et al. 2009; Zhang et al. 2012). Despite its high expression level in the brain, knockout (KO) mice develop normally and present only mild behavioral abnormalities (Lamprianou et al. 2006). RPTP $\gamma$  was not normally found in cortical astrocytes (Lamprianou et al. 2006), however its transcription can be induced by IL1 and TNF $\alpha$  in human astrogloma cell lines *in vitro* (Schumann et al. 1998).

Despite being mainly a neuronal protein, a thorough analysis of RPTP $\gamma$  distribution in the adult brain has been described using a knock-in mice where the promotor of RPTP $\gamma$  drive LacZ expression (Lamprianou et al. 2006). However this analysis did not allow the possibility to distinguish between the various isoforms of RPTP $\gamma$ . Importantly, at least 4 distinct RPTP $\gamma$  isoforms exist, including a truncated soluble PTP (sPTP $\gamma$ ), that lacks the intracellular catalytic C-terminal domains and it is thus devoid of the phosphatase activity (Shintani et al. 1997). One of the

limitations in studying different RPTP $\gamma$  isoforms is the scarceness of antibodies against different specific epitopes, especially toward the extracellular N-terminal region.

In this study we used different antibodies against C- and N-terminal epitopes, the last ones developed in our laboratory, in order to investigate the distribution of the intra- and of the extracellular domains of RPTP $\gamma$ , with the aim of evaluating whether specific isoforms (Sorio et al. 1995; Mafficini et al. 2007; Vezzalini et al. 2007) could be detectable in tissues. Moreover we investigated the consequence of neuroinflammation on its expression.

We found RPTP $\gamma$  expression in the neuropil of cortical neurons and in cerebellar Bergmann radial glia, whereas a truncated form lacking the C-terminal domain was present in the soma of cortical and hippocampal neurons, in Purkinje cells and interneurons of the cerebellar cortex. We also found that astrocytes upregulated both the full length and the truncated RPTP $\gamma$  isoform during neuroinflammation.

Overall our study highlights a role for RPTP $\gamma$  during astrocyte activation *in vivo* and highlight for the first time in situ a differential distribution of the C- and N-terminal portions, suggesting a complex post-translational regulation of RPTP $\gamma$  in the adult nervous system.

## **Materials and Methods**

### *Animals*

Mice were maintained under standard environmental conditions (temperature, humidity, 12 h/12 h light/dark cycle, with water and food *ad libitum*) under veterinarian assistance. Animals handling and surgery were performed following a protocol which received approval by the Animal Care and Use Committee of the University of Verona (CIRSAL), and authorization by the Italian Ministry of Health, in strict adherence to the European Communities Council (86/609/EEC) directives, minimizing the number of animals used and avoiding their suffering.

We used adult C57/BL6J mice purchased from Harlan. 5 months old 5XFAD mice were purchased from the Jackson Laboratory (Bar Harbor, Maine). **Adult RPTP $\gamma$  deficient mice (129SveV) were generously given by Dr. S Harroch from the Institut Pasteur of Paris, France.**

### *Immunofluorescence.*

Under deep anesthesia (tribromoethanol, intraperitoneal dose of 0,5 g/kg body weight) mice were transcardially perfused with paraformaldehyde 4% in saline buffer. The brain was excised, postfixed and cryoprotected before freezing. Brain slices (35 $\mu$ m thick) were obtained and stained with antibodies. Some mice were intraperitoneal (ip) injected with 500 $\mu$ g/kg of LPS (Life Technologies) and sacrificed 24h post injection.

Free floating cryosections were stained with different combinations of antibodies. Sections were permeabilized with the following solution: 2% Bovine Serum Albumin and 0,3% Triton X-100 in PBS, pH 7.4 for 30 minutes. Then sections were incubated overnight at 4°C with primary antibodies followed by the proper secondary Alexa Fluor-conjugated antibodies (1:1000, Life Technologies) for 1h at RT. Nuclei were stained with DAPI (Sigma). After mounting with an anti-fading solution, slices were studied by fluorescence microscopy (DM6000B, Leica Microsystem) and confocal microscopy (TCS-SP5, Leica Microsystem).

### *Antibodies*

The specificity of antibodies against N-terminus domain of Ptp<sup>prg</sup>-RPTP $\gamma$ : chicken anti-RPTP $\gamma$  (ch-RPTP $\gamma$ ) and rabbit anti-RPTP $\gamma$  (rb-RPTP $\gamma$ -P4) used in this study were previously described in detail (Sorio et al. 1995; Mafficini et al. 2007; Vezzalini et al. 2007, Della Peruta et al., 2010 Cancer Research). We also used anti-RPTP $\gamma$  C-terminus domain developed in goat (goat-RPTP $\gamma$  1:20 Santa Cruz) and anti-PTP $\zeta$ , (mouse IgG1, 1:250, BD Bioscience). The features of anti-RPTP $\gamma$  antibodies, together with the epitope localizations are given in Table 1.

Neuronal and glial markers used were: anti-MAP2 (mouse IgG1, 1:1000, Sigma-Aldrich), anti-NeuN (mouse IgG1, 1:200, Chemicon), anti- $\beta$ III-tubulin (Rabbit, 1:1000, Sigma-Aldrich), anti-Amyloid  $\beta$  clone 4G8 (IgG2b, 1:200, Covance), anti-Calbindin (IgG1, 1:500, Swant), anti-GFAP (IgG1, 1:500, Chemicon), anti-S100 (Rabbit, 1:400, Dako) and anti-CD11b (rat, 1:1000, Serotec).

### *Tissue lysate*

C57 mice were sacrificed by terminal anesthesia 24h after LPS or saline ip injection. After a transcardial perfusion with PBS/Heparin in order to discard the blood, brain cortices were quickly removed, frozen in liquid nitrogen vapor and stored at -80°C. Brain cortices were cut by cryostat and 30  $\mu$ m sections were homogenized in lysis buffer (LB) containing 50 mM Tris (pH 7.4), 1% Triton X-100, 150 mM NaCl, 200  $\mu$ M NaVO<sub>4</sub>, 1 mM EDTA, 1 mM DTT, 1 mM NaF and Complete EDTA-free Protease Inhibitor Cocktail Tablets (Roche, Germany), incubated for 20 min in a rotating wheel at 4°C and then centrifuged for 15 min at 4 °C at 15000  $\times$ g in a Biofuge Pico (DJB Labcare Ltd. UK). All the lysis procedures were carried out at 4°C.

### *Western Blot*

After protein quantification by Bradford assay, equal amounts of protein were resuspended in sample buffer (SB: 40 mM Tris-HCl pH 6.8, 183 mM  $\beta$ -mercaptoethanol, 1% SDS, 5% glycerol) and denatured at 95°C for 10 minutes. Lysates were resolved on 7,5 % SDS-PAGE and electroblotted onto polyvinylidene difluoride membrane (Millipore Corp., Bedford, MA). The

membrane was blocked with 5% BSA in TBS containing 0.05 % Tween-20 (TBST) for anti-GFAP (1:1000), and 5% skimmed milk for rb-RPTP $\gamma$ -P4 (1 $\mu$ g/ml) in 1% BSA TBST buffer overnight. After washes in TBST, the membrane was incubated with rabbit anti-goat-HRP (Sigma-Aldrich) or goat anti-mouse-HRP (GE Healthcare, Little Chalfont, UK) for 1 h. After washing with TBST, the signal was detected with the enhanced chemiluminescence kit (Millipore Corp., Bedford, MA) using an ImageQuant LAS 4000 (GE healthcare) imager. Band intensity was detected by Quantity One software (Biorad) and normalized to Ponceau Red staining.

## Results

### *1- RPTP $\gamma$ is a neuronal protein of widespread distribution in the adult mouse brain.*

In order to investigate the expression and distribution of RPTP $\gamma$  and related isoforms in the adult mouse brain, we stained brain sections with antibodies against either the extracellular N-terminal domain or the intracellular C-terminal portion. To detect the extracellular N-terminal domain we used antibodies made in chicken and developed in our laboratory (Vezzalini et al. 2007). Moreover, we used neuronal and glial markers to identify the different cell type. As shown in figure 1, we found that RPTP $\gamma$  was widely distributed throughout the brain, with immunopositivity in many neurons of the cerebral cortex and in the hippocampus. Its distribution was mainly neuronal, as demonstrated by  $\beta$ III-tubulin colocalization (Fig. 1 a-c). Astrocyte positivity was dependent on cell size and on the degree of Glial Fibrillary Acidic Protein (GFAP) expression: small astrocytes with thin GFAP-positive processes were negative to RPTP $\gamma$  (Fig. 1 j-l), whereas bigger astrocytes, such as those of the hippocampus (Fig. 1 d-f and m) or perivascular astrocytes (Fig. 1 g-i), with thick GFAP-positive processes were generally positive to RPTP $\gamma$ . Microglial cells were negative (Fig. 1 n-o).

In the cerebellum (Fig. 2), RPTP $\gamma$  positivity was found in the molecular layer, in Purkinje cells (soma and main dendrites but not in spiny branchlets) and interneurons as demonstrated by colocalization with  $\beta$ III-tubulin. Colocalization with the radial glial markers S100 and GFAP in the cerebellar cortex revealed a RPTP $\gamma$  positivity of Bergmann glial cells, the radial glia of the cerebellum. Almost all deep cerebellar nuclei were also strongly positive (not shown).

Using the fluorescence microscope we performed an atlas-based analysis of some coronal sections at different distances from the bregma, and we found that RPTP $\gamma$  was widely expressed in many structures throughout the brain. Results are summarized in Table 2. RPTP $\gamma$  immunoreactivity was present in different layers of the cerebral cortex, in the striatum, in many nuclei of the thalamus and of the brainstem, and it was generally a neuronal protein in the normal

adult mouse brain. Many elements of the white matter were negative, except for some big astrocytes. The wide distribution of RPTP $\gamma$  suggests that it may have a role in the building or maintenance of synaptic circuitry in the brain.

Differential labeling and confocal analysis of the C- and N-terminal domain epitopes show that the two portions of the phosphatase colocalize in the neuropil, but not in the soma of neurons, in which the N-terminal epitope positivity was mainly found (Fig. 3). Interestingly, in the cerebellum the two portions colocalize in Bergmann glial cells, thus indicating the presence of a full length RPTP $\gamma$  isoform. The N-terminal positivity was found alone in Purkinje cells and cerebellar interneurons, indicating the presence of truncated forms.

These data shows that distinct isoforms of RPTP $\gamma$  are present in different types of neurons/glia cells of the brain in physiological conditions.

We also performed a staining on a few slices of one heterozygous and one RPTP $\gamma$  KO mouse (Lamprianou et al. 2006). Despite some residual staining remained, we observed a strong reduction of the RPTP $\gamma$  positivity as compared to the heterozygous control (see supplementary figure).

## *2- RPTP $\gamma$ and RPTP $\zeta$ , expressions are distinct*

RPTP $\gamma$  and RPTP $\zeta$ , are members of the same family of tyrosine phosphatases and are highly homologous. To assess the specificity of our antibodies against RPTP $\gamma$ , we stained sections simultaneously for RPTP $\gamma$  and RPTP $\zeta$ , which resulted in a distinct staining pattern. Both proteins were neuronal, but RPTP $\zeta$  was observed as a spotted labeling along the neuropil both in the cortex and in the hippocampus (Fig. 4). Indeed the antibody anti- RPTP $\zeta$  recognizes the intracellular C-terminal phosphatase domain and therefore is able to detect 2 out of 3 RPTP $\zeta$  isoforms. A strong neuronal post-synaptic signal was previously reported by using this antibody together with a lack of positivity in cortical and hippocampal astrocytic processes (Hayashi et al. 2005). Thus it is not surprising that in our sections hippocampal astrocytes were negative for RPTP $\zeta$  (Fig. 4 i). In the cerebellum RPTP $\zeta$  was found only in Purkinje cell dendrites, but not in radial glia (Fig. 4 j-l). Our data show that the staining for RPTP $\zeta$ , and RPTP $\gamma$  in neurons were distinct and only partially overlapping, thus supporting the specificity of our antibodies against RPTP $\gamma$  and suggesting that the two proteins can be expected to have different and specific functions in neurons, even if they are highly homologous.

## *3- RPTP $\gamma$ distribution in inflammatory states: LPS and AD*

The expression of RPTP $\gamma$  in protoplasmic astrocytes with thick GFAP-positive branches under physiological conditions prompted us to investigate whether its expression could increase in brain during inflammation. Thus, we performed the staining of brain sections in mice sacrificed 24 h after LPS ip injection, a treatment that is known to cause a general brain inflammation and glial cell activation within 24 h from injection (Kwon et al. 2010). We found that activated GFAP-positive cortical astrocytes were strongly positive for RPTP $\gamma$ , while the protein distribution in neurons did not change significantly (Fig. 5 a to d). In order to quantify this phenomenon, we performed western blotting experiments on cerebral cortices of adult mice with or without LPS injections. As shown in Fig. 5 e, the increase of GFAP reflects the increase of activation state of astrocytes 24h after LPS treatment. We also performed western blotting using an anti-RPTP $\gamma$  antibody made in rabbit (Rb-RPTP $\gamma$ -P4) (Sorio et al. 1995), that revealed an increase, upon LPS treatment, of all the 3 isoforms detected: the full length RPTP $\gamma$  (180kDa band) and two truncated isoforms at 120 and 80kDa bearing the extracellular N-terminal portion that is recognized by the above mentioned antibody (Fig. 5 e). Interestingly, the densitometry revealed that after LPS the 120 kDa band, increased much more than the others (180 kDa) ( $p < 0,01$  by t-test). Moreover the normalized expression level of the isoforms remained linearly correlated among the 3 individual mice, with a  $r^2$  from of 0.67 to 0.77 (Fig 5 g to i), suggesting that the smaller isoforms might derive from proteolytic cleavage of the longers. As gel loading control the Ponceau staining is also shown.

We further confirmed that activated astrocytes express high levels of RPTP $\gamma$  in another model of brain inflammation: the 5XFAD mouse, one of the murine models of Alzheimer's disease (Oakley et al. 2006). We stained cerebral sections of a 6 months old mouse in order to detect amyloid plaques in the cerebral cortex by using the 4G8 antibody. This antibody labels amyloid  $\beta$  and its precursors such as the neuronal Amyloid Precursor Protein (APP), which are ubiquitously expressed in neurons. For this reason many neurons are positive for 4G8 staining (Fig. 6). In tissue sections the amyloid plaques are clearly recognizable by their morphology. The strong activation of astrocytes and microglia around the amyloid plaques is visualized by the cell morphology (astrocytes here are bigger and present thick processes) and the elevation of the specific markers GFAP and Cd11b. Also, in this model of neuroinflammation, neurons and astrocytes were strongly positive for RPTP $\gamma$ . On the contrary, both activated microglial cells and amyloid plaques were negative.

All together these data suggest that RPTP $\gamma$  is generally upregulated during neuroinflammation *in vivo* and might play a role in astrocyte activation.

## Discussion

In this study we investigated the distribution of RPTP $\gamma$  and related isoforms in the nervous system by using, for the first time in the literature, simultaneously antibodies against C- and N-terminus epitopes of the protein. These antibodies are able to distinguish between the full length (colocalization of C- and N- terminus) and the truncated isoforms lacking C-terminus domain (only N-terminus positivity) of the phosphatase. In line with previous studies (Lamprianou et al. 2006), we found a predominant and widespread neuronal RPTP $\gamma$  immunopositivity throughout the brain. Using the C- and N-terminus antibodies, we further analyzed the expression of RPTP $\gamma$ : both N- and C-terminus were found in the neuropil of cortical and hippocampal neurons demonstrating a RPTP $\gamma$  full length expression. The positivity for the N-terminal domain was found also in the soma, often without its C-terminal counterpart showing an expression of a shorter isoform in the soma. Thus, at least two isoforms of RPTP $\gamma$  are present in the adult normal murine brain and are differentially distributed not only in different types of neurons, but also in different compartments of the same cell. Clarifying whether the truncated N-terminal isoforms are produced by alternative splicing or by proteolytic cleavage starting from the full-length protein, will be object of further studies. Indeed a proteolytic cleavage *in vivo* have been already hypothesized, but not yet demonstrated, studying the changes in RPTP $\gamma$  expression during mouse development in the superior colliculus: here three different isoforms were detected at different time points from E13 to P20 (Reinhard et al. 2009).

It was reported that RPTP $\gamma$  KO mice did not show any obvious phenotype, displaying only minor behavioral changes, in spite of the expression during development and in the adult brain in pyramidal and sensory neurons (Lamprianou et al. 2006; Zhang et al., 2012). Indeed RPTP $\gamma$  is highly homologous to RPTP $\zeta$ , and both are expressed in neurons (Shintani et al. 1998; Tanaka et al. 2003; Hayashi et al. 2005), suggesting that potentially they might have overlapping activities at the occurrence and RPTP $\zeta$ , could compensate the loss of RPTP $\gamma$ . We stained our sections simultaneously for RPTP $\gamma$  and for RPTP $\zeta$ , and found only partial overlapping signals in neurons and, an overall different staining pattern. Beside supporting the specificity of the antibodies against the N-terminal portion of RPTP $\gamma$  these results suggest that PTPs other than RPTP $\zeta$  might compensate for RPTP $\gamma$  loss during the embryonal development of KO mice.

This report supports the previous studies on the pattern of expression of RPTP $\gamma$  and RPTP $\zeta$ . Despite it is reported that RPTP $\zeta$  is strongly expressed in glial cells (oligodendrocytes and astrocytes) we found a spotted-like positivity in cortical and hippocampal neurons, in line with previous studies that used the same antibodies (Hayashi et al. 2005), while RPTP $\gamma$  had a very strong expression in neurons (Lamprianou et al, 2006). We show that most perivascular astrocytes

do not express RPTP $\gamma$  in normal adult mouse brain, and that in some sublocalisation of neurons both RPTP $\zeta$  and RPTP $\gamma$  can be detected.

The RPTP $\gamma$  role and function in the adult CNS is unknown and largely unexplored, as well as are its ligands. RPTP $\gamma$  could putatively bind to contactins-3, -4 and -5 that are widely distributed in the adult brain, but the meaning of this interaction is unclear (Bouyain and Watkins 2010; Lamprianou et al. 2011; Hendriks et al. 2013). Some recent data support a function of RPTP $\gamma$  in depression (Zhang et al. 2012) and bipolar disorders (Hamshere et al. 2009). This is in line with its potential interaction with the CNTNs and CNTNs signaling pathway, which are genes mutated in mental disorders (Cottrel et al. 2011).

In chick spinal cord RPTP $\gamma$  plays a role in spinal cord neurogenesis during embryonic development, where it appears to influence the Wnt/ $\beta$  catenin signaling and neuronal survival (Hashemi et al. 2011). Moreover RPTP $\gamma$  inhibits the NGF-mediated neurite outgrowth in PC12 cells (Shintani et al. 2001). Our study is the first that describes the distribution of different RPTP $\gamma$  isoforms in the brain, and it completes and enriches the current knowledge about the distribution of RPTP $\gamma$  and could help in developing new hypotheses about its role and molecular mechanisms in neurons of the adult brain.

Another major finding of our study is that, despite not being expressed in small astrocytes, RPTP $\gamma$  is up-regulated in these same cells following intraperitoneal injection of LPS and in the 5XFAD murine model of Alzheimer's disease, two well characterized *in vivo* models of brain inflammation. These data suggest, for the first time *in vivo*, that RPTP $\gamma$  can be involved in the process of astrocyte activation. It is already known that, after Interleukin 1  $\beta$  (IL1  $\beta$ ) and Tumor Necrosis Factor alpha (TNF $\alpha$ ) treatment *in vitro*, RPTP $\gamma$  mRNA is upregulated by human astrocytoma cells (Schumann et al. 1998). Indeed after LPS ip treatment both IL1  $\beta$  and TNF $\alpha$  mRNA are upregulated in mouse brain within 90min, and the astrocyte activation reaches its maximum at 24h post injection (Kwon et al. 2010). In this study we showed that 24h after LPS injection the increase in GFAP level is accompanied by the increase in RPTP $\gamma$  protein level in brain astrocytes. This is the first time that this increase is demonstrated *in vivo* on different isoforms of RPTP $\gamma$ . Indeed, we observed a marked increase of the 120 kDa truncated RPTP $\gamma$  isoform by WB after LPS treatment. Since all isoforms present a reciprocal linear correlation, it might be possible that the truncated isoforms are produced in part by cleavage starting from the longer ones. Interestingly following LPS treatment, activated microglia and astrocytes are known to produce many different matrix metalloproteases like MMP-3 and MMP-9 (Gottschall and Deb 1996; Lee et al. 2003). Cytokines like IL1  $\beta$  and TNF $\alpha$  are potent stimulant of MMPs production by activated glia *in vitro* (Gottschall and Yu 1995; Crocker et al. 2006; for a review see Candelario-Jalil et al. 2009). The possible role of matrix metalloproteases in the cleavage of

RPTP $\gamma$  during neuroinflammation will be object of further studies. Indeed we cannot exclude that short and long isoforms are produced by alternative splicing, as happens for RPTP $\zeta$ , that is highly homologous to RPTP $\gamma$ .

As concern the RPTP $\zeta$  signal, we found a punctuate staining pattern in neurons, in line with previous studies where this protein was found to be localized post-synaptically and not in astrocytes when the same antibody was used (Hayashi et al. 2005; Kawachi et al. 1999). It has been reported for long time that RPTP $\zeta$  is expressed in astrocytes (Canoll et al. 1996; Sakurai et al. 1996;). Among the three splicing variants, its soluble isoform phosphacan lacking the intracellular domain is released during inflammation or lesion (Faissner et al. 2006). A possible explanation for this lack of positivity in astrocytes might be that mature astrocytes preferentially express the phosphacan isoform (Canoll 1996 et al.; Sakurai 1996 et al.), which is not detected by this antibody.

More recent studies suggest that the neuronal RPTP $\zeta$  isoforms might play a critical role in the reactive synaptogenesis occurring after injury (Harris et al., 2011). Indeed the last decade of research on Phosphacan/RPTP $\zeta$  isoforms reveals a high degree of complexity in the regulation and roles of this particular phosphatase in both physiological and pathological conditions (Lamprianou et al. 2011; Hendriks et al. 2013).

In this study, we show an increased expression of the RPTP $\gamma$  isoform lacking the D2 domain upon inflammation. RPTP $\gamma$  inhibits NGF signaling and therefore TRK dependent axon growth (Shintani 2001). Using different signaling pathways, RPTP $\zeta$  and RPTP $\gamma$  could generate similar biological function such as modulating neurite outgrowth during inflammation. The increased expression of the RPTP $\gamma$  isoform lacking a C-terminal portion, likely including the D2 domain, is of interest. Indeed structural biology of PTPs proposed that these proteins homodimerize inducing inhibition of the phosphatase activity by changing the relative position of the D1 and D2 domains (Tremblay 2009; Barr et al. 2009). Thus, an isoform lacking the D2 domain could not be inhibited by this mechanism and could strengthen its efficacy to dephosphorylate the NGF/TRK signaling or other still unidentified pathways.

In this line both phosphatase RPTP $\gamma$  and RPTP $\zeta$  should increase in astrocytes when inflammation occurs. Indeed, as one of the main components of Chondroitin Sulfate Proteoglycans (CSPGs), phosphacan is expressed at high level by reactive astrocytes upon injury, and prevent axon growth by direct binding to the surface of the growth cone and by interacting with L1/NgCAM/laminin substrates (for a review see Sandvig et al., 2004). RPTP $\gamma$  is also expressed upon cytokines treatment and inflammation. If both phosphatases have only partial overlap of expression, they might address similar biological function.

Overall, our study enriches the current knowledge about the role of RPTP $\gamma$  in astrocyte activation *in vivo* and the differential distribution of RPTP $\gamma$  isoforms could help in making new hypothesis about the mechanism of action/role of the phosphatase in neuronal physiological functions.

#### ACKNOWLEDGEMENTS

This work was supported by University of Verona and Fondazione Cariverona-project Verona Nanomedicine Initiative. Development and characterization of antibodies were supported by AIRC IG 4667 and Consorzio per gli Studi Universitari, Verona.

Conflict of Interest: The authors declare no competing financial interests.

#### Figure Legends

##### **Fig. 1 RPTP $\gamma$ is expressed in neurons and in some astrocytes in the adult brain.**

Examples of immunostaining showing the RPTP $\gamma$  positivity of neurons (a-c), astrocytes and microglia (d-o). Colocalization of RPTP $\gamma$  (green) and  $\beta$ III-tubulin (blue) shows the neuronal expression of RPTP $\gamma$  in the cerebral cortex (a-c). Astrocytes are labeled by GFAP (red). In a and c astrocytes surrounding a blood vessel are also shown (red).

A representative image of the dentate gyrus shows the mild colocalization of RPTP $\gamma$  and GFAP, indicating the positivity of some astrocytes in the hippocampus (d-f) as well as those surrounding some blood vessels (g-i). Small astrocytes (j-l) are negative for RPTP $\gamma$ , whereas a mild positivity was found only in some big astrocytes (GFAP red in m) but not in the resting microglia labeled by CD11b (red in n and o). In some images the nuclear DAPI staining is also shown. Scale bars 50 $\mu$ m in a to f, 20 $\mu$ m in g to o.

##### **Fig. 2 RPTP $\gamma$ is expressed in neurons of the cerebellar molecular layer and in cerebellar radial glia.**

Immunostaining showing the RPTP $\gamma$  expression in the cerebellar cortex of adult mouse brain. (a-d) Colocalization of RPTP $\gamma$  (green) and  $\beta$ III-tubulin (red) shows positivity for interneurons of the molecular layer, as well as Purkinje cell main dendrite. e-h. Colocalization of RPTP $\gamma$  and GFAP (red) shows positivity for Bergmann radial glia. g and h are enlargements of the boxed region in f. (i-l) Colocalization of RPTP $\gamma$  and the Bergmann glia specific marker S100 (red) confirms the expression of RPTP $\gamma$  in these cells. k is an enlargement of the boxed region in j. In some images nuclei counterstaining by DAPI (blue) is also shown. ML: molecular layer; PL: Purkinje cell layer; GCL: granule cell layer. Scale bars 20 $\mu$ m in g, h, k, l, 40 $\mu$ m in all the other images.

**Fig. 3 RPTP $\gamma$  C- and N-terminal epitopes are differently localized within brain cells.**

Immunostaining of brain sections by using different antibodies against either the N- (anti-RPTP $\gamma$  chicken isotype, green) or the C-terminal (red) portion of RPTP $\gamma$  allows to distinguish between the full length protein (colocalization) and a truncated isoform lacking the C-terminus epitope (green only). (a-b) cerebral cortex shows that the N- and C-terminus colocalizes in the apical dendrite and in some neurons, but the soma mainly presents the N-terminus positivity alone. (c-d) enlargements of the boxed region in a. (e-h) shows that resting astrocytes (GFAP, blue) are negative for both epitopes. (i-l) Cerebellar cortex displays C- and N- terminus colocalization only in Bergamnn radial glia, whereas the N-terminal epitope is present alone in Purkinje cells and colocalizes with Calbindin (blue). ML: molecular layer; PL: Purkinje cell layer. Scale bars 30 $\mu$ m in a, b, i, j, k, l; 15 $\mu$ m in c, d, e, f, g, h.

**Fig. 4 Comparison of the distribution of RPTP $\zeta$  and RPTP $\gamma$  receptors.**

Immunostaining of brain sections by using anti-RPTP $\gamma$  (antibody made in chicken) and anti-RPTP $\zeta$ , a protein that is highly homologous with RPTP $\gamma$ . a-f Cerebral cortex, where colocalization of RPTP $\gamma$  (green) and RPTP $\zeta$ , (red) occurs in the neuropil ( $\beta$ III-tubulin, blue). f is an enlargement of the boxed region in d and shows the spotted staining pattern of RPTP $\zeta$ . g-i In the hippocampus both proteins are neuronal. The boxed region enlarged in i shows astrocytes that are negative for RPTP $\zeta$  (arrows). j-l In the cerebellar cortex RPTP $\zeta$  was found in Purkinje cell primary dendrites where it partially colocalizes with RPTP $\gamma$ .

The different localizations and staining patterns of RPTP $\zeta$ , and RPTP $\gamma$  further support the specificity of our N-terminal antibodies against RPTP $\gamma$  N-terminal domain. ML: molecular layer; PL: Purkinje cell layer. Scale bars 30 $\mu$ m.

**Fig. 5 RPTP $\gamma$  expression increases in astrocytes after LPS injection.**

RPTP $\gamma$  expression in mouse brain cortex 24h after LPS i.p. injection was assessed by immunostaining and WB. (a-d) Immunostaining showing a strong positivity for RPTP $\gamma$  (green) in activated astrocytes (GFAP, red; colocalization yellow). The boxed region of a is enlarged in b, c and d, in order to highlight activated astrocytes surrounding a blood vessel. Scale bars 30 $\mu$ m. (e) WB of brain cortex lysates of 3 normal (-) and 3 LPS (+) treated mice. Band intensity of RPTP $\gamma$  was detected by an antibody made in rabbit (rb-RPTP $\gamma$ -P4). Bands at 180kDa show the full length protein isoform, whereas at 120 and 80 kDa we found two truncated isoforms. GFAP increase confirms the astrocyte activation after LPS injection. Ponceau staining was used for normalization of the loaded protein. The densitometry plot (f) shows the normalized band intensity relative to 120 and 180kDa isoforms with or without LPS treatment. All isoforms increased after LPS

treatment, especially the truncated 120kDa RPTP $\gamma$ .  $p < 0,01$  by t-test. (g-i) Plots showing the strong linear correlation between the normalized intensities of the 3 RPTP $\gamma$  isoforms showed in e, suggesting their origin from a common precursor.

**Fig. 6 RPTP $\gamma$  is expressed in cortical activated astrocytes in the murine model of Alzheimer's disease.**

Expression of RPTP $\gamma$  (green) was assessed in brain cortex of a 6 month old 5xFAD mouse brain by immunostaining. Staining for amyloid  $\beta$  peptide (4G8, red) shows neuronal APP and amyloid plaques (red). (a-b) RPTP $\gamma$  (green) is neuronal, but a strong positivity was found also in astrocytes (GFAP, blue in a, red in b, false color). (c) shows the colocalization of RPTP $\gamma$  (green) and 4G8 (red) in neurons but not in amyloid plaques. (d-f) Activated microglia (CD11b, red) surrounding amyloid plaques is negative for RPTP $\gamma$ . (f) represents an enlargement of the boxed region in d. (g-i) Neuronal expression of RPTP $\gamma$  in AD mice assessed by colocalization with MAP2 (blue in g and red in h, false color). Scale bars 40  $\mu\text{m}$  in a-e, 20  $\mu\text{m}$  in f-i.

**Supplementary figure**

As an additional test for antibody specificity we stained some slides from one heterozygous and one RPTP $\gamma$  KO mouse using the two antibodies against the N- (ch-RPTP $\gamma$ , green) and the C-terminus (goat-RPTP $\gamma$ , red) epitopes of the phosphatase. Cerebral cortex (A-F and J-O) and hippocampus (G-I and P-R) showed a strong decrease of RPTP $\gamma$  signal in the KO (J to R) in comparison to the heterozygous (A to I). A residual staining was still present in some regions, in particular in the granular layer of the hippocampus, a region known to be prone to aspecific staining. Scale bars 50 $\mu\text{m}$ .

**Table 1**

Schematic representation of the antibodies used against RPTP $\gamma$ . Epitopes: amino acid number of epitopes, validated application: IP= immuno-precipitation, WB= western blot, IHC= immuno histo chemistry, Flow= flow cytometry, IF= immuno fluorescence. The RPTP $\gamma$  structure scheme displays where the epitopes are localized within the predicted protein sequence of the 4 different isoforms. CA: Carbonic anhydrase-like; FNIII: Fibronectin type III-like domain; TM: transmembrane portion; D1: active phosphatase domain and D2: inactive phosphatase domain.

**Table 2**

Distribution of RPTP $\gamma$  positivity in mouse brain coronal sections, assessed by immunostaining and fluorescence microscopy.

## References

- Barnea G, Silvennoinen O, Shaanan B, Honegger AM, Canoll PD, D'Eustachio P, Morse B, Levy JB, Laforgia S, Huebner K, et al. (1993) Identification of a carbonic anhydrase-like domain in the extracellular region of RPTP gamma defines a new subfamily of receptor tyrosine phosphatases. *Mol Cell Biol* 13 (3):1497-1506
- Barr, A. J., Ugochukwu, E., Lee, W. H., King, O. N., Filippakopoulos, P., Alfano, I., et al. (2009). Large-scale structural analysis of the classical human protein tyrosine phosphatome. [Research Support, Non-U.S. Gov't]. *Cell*, 136(2), 352-363, doi:10.1016/j.cell.2008.11.038.
- Bouyain S, Watkins DJ (2010) The protein tyrosine phosphatases PTPRZ and PTPRG bind to distinct members of the contactin family of neural recognition molecules. *Proc Natl Acad Sci U S A* 107 (6):2443-2448. doi:0911235107 [pii] 10.1073/pnas.0911235107
- Candelario-Jalil E, Yang Y, Rosenberg GA (2009) Diverse roles of matrix metalloproteinases and tissue inhibitors of metalloproteinases in neuroinflammation and cerebral ischemia. *Neuroscience* 158 (3):983-994. doi:S0306-4522(08)00895-6 [pii] 10.1016/j.neuroscience.2008.06.025
- Canoll, P. D., Petanceska, S., Schlessinger, J., & Musacchio, J. M. (1996). Three forms of RPTP-beta are differentially expressed during gliogenesis in the developing rat brain and during glial cell differentiation in culture. [Research Support, U.S. Gov't, P.H.S.]. *J Neurosci Res*, 44(3), 199-215, doi:10.1002/(SICI)1097-4547(19960501)44:3<199::AID-JNR1>3.0.CO;2-B.
- Cottrell, C. E., Bir, N., Varga, E., Alvarez, C. E., Bouyain, S., Zernzach, R., et al. (2011). Contactin 4 as an autism susceptibility locus. [Case Reports Research Support, N.I.H., Extramural Research Support, U.S. Gov't, Non-P.H.S.]. *Autism Res*, 4(3), 189-199, doi:10.1002/aur.184.
- Crocker SJ, Milner R, Pham-Mitchell N, Campbell IL (2006) Cell and agonist-specific regulation of genes for matrix metalloproteinases and their tissue inhibitors by primary glial cells. *J Neurochem* 98 (3):812-823. doi:JNC3927 [pii] 10.1111/j.1471-4159.2006.03927.x
- Dabrowski A, Umemori H (2011) Orchestrating the synaptic network by tyrosine phosphorylation signalling. *J Biochem* 149 (6):641-653. doi:mvr047 [pii] 10.1093/jb/mvr047

- Della Peruta M, Martinelli G, Moratti E, Pintani D, Vezzalini M, Mafficini A, Grafone T, Iacobucci I, Soverini S, Murineddu M, Vinante F, Tecchio C, Piras G, Gabbas A, Monne M, Sorio C (2010) Protein tyrosine phosphatase receptor type  $\{\gamma\}$  is a functional tumor suppressor gene specifically downregulated in chronic myeloid leukemia. *Cancer research* 70 (21):8896-8906. doi:10.1158/0008-5472.CAN-10-0258
- Faissner A, Heck N, Dobbertin A, Garwood J (2006) DSD-1-Proteoglycan/Phosphacan and receptor protein tyrosine phosphatase-beta isoforms during development and regeneration of neural tissues. *Adv Exp Med Biol* 557:25-53. doi:10.1007/0-387-30128-3\_3
- Gottschall PE, Deb S (1996) Regulation of matrix metalloproteinase expressions in astrocytes, microglia and neurons. *Neuroimmunomodulation* 3 (2-3):69-75
- Gottschall PE, Yu X (1995) Cytokines regulate gelatinase A and B (matrix metalloproteinase 2 and 9) activity in cultured rat astrocytes. *J Neurochem* 64 (4):1513-1520
- Hamshere, M. L., Green, E. K., Jones, I. R., Jones, L., Moskvina, V., Kirov, G., et al. (2009). Genetic utility of broadly defined bipolar schizoaffective disorder as a diagnostic concept. [Comparative Study Research Support, Non-U.S. Gov't]. *Br J Psychiatry*, 195(1), 23-29, doi:10.1192/bjp.bp.108.061424.
- Harris, J. L., Reeves, T. M., & Phillips, L. L. (2011). Phosphacan and receptor protein tyrosine phosphatase beta expression mediates deafferentation-induced synaptogenesis. [Research Support, N.I.H., Extramural]. *Hippocampus*, 21(1), 81-92, doi:10.1002/hipo.20725.
- Hashemi H, Hurley M, Gibson A, Panova V, Tchetchelnitski V, Barr A, Stoker AW (2011) Receptor tyrosine phosphatase PTPgamma is a regulator of spinal cord neurogenesis. *Mol Cell Neurosci* 46 (2):469-482. doi:S1044-7431(10)00263-0 [pii] 10.1016/j.mcn.2010.11.012
- Hayashi N, Oohira A, Miyata S (2005) Synaptic localization of receptor-type protein tyrosine phosphatase zeta/beta in the cerebral and hippocampal neurons of adult rats. *Brain Res* 1050 (1-2):163-169. doi:S0006-8993(05)00787-0 [pii] 10.1016/j.brainres.2005.05.047
- Hendriks, W. J., Elson, A., Harroch, S., Pulido, R., Stoker, A., & den Hertog, J. (2013). Protein tyrosine phosphatases in health and disease. *FEBS J*, 280(2), 708-730, doi:10.1111/febs.12000.
- Johnson KG, Van Vactor D (2003) Receptor protein tyrosine phosphatases in nervous system development. *Physiol Rev* 83 (1):1-24. doi:10.1152/physrev.00016.2002

- Kawachi, H., Tamura, H., Watakabe, I., Shintani, T., Maeda, N., & Noda, M. (1999). Protein tyrosine phosphatase zeta/RPTPbeta interacts with PSD-95/SAP90 family. [Research Support, Non-U.S. Gov't]. *Brain Res Mol Brain Res*, 72(1), 47-54.
- Kwon MS, Seo YJ, Choi SM, Won MH, Lee JK, Park SH, Jung JS, Sim YB, Suh HW (2010) The time-dependent effect of lipopolysaccharide on kainic acid-induced neuronal death in hippocampal CA3 region: possible involvement of cytokines via glucocorticoid. *Neuroscience* 165 (4):1333-1344. doi:S0306-4522(09)01971-X [pii]  
10.1016/j.neuroscience.2009.11.060
- Lamprianou S, Chatzopoulou E, Thomas JL, Bouyain S, Harroch S (2011) A complex between contactin-1 and the protein tyrosine phosphatase PTPRZ controls the development of oligodendrocyte precursor cells. *Proc Natl Acad Sci U S A* 108 (42):17498-17503. doi:1108774108 [pii]  
10.1073/pnas.1108774108
- Lamprianou S, Harroch S (2006) Receptor protein tyrosine phosphatase from stem cells to mature glial cells of the central nervous system. *J Mol Neurosci* 29 (3):241-255. doi:JMNM:29:3:241 [pii]  
10.1385/JMNM:29:3:241
- Lamprianou S, Vacaresse N, Suzuki Y, Meziane H, Buxbaum JD, Schlessinger J, Harroch S (2006) Receptor protein tyrosine phosphatase gamma is a marker for pyramidal cells and sensory neurons in the nervous system and is not necessary for normal development. *Mol Cell Biol* 26 (13):5106-5119. doi:26/13/5106 [pii]  
10.1128/MCB.00101-06
- Lee WJ, Shin CY, Yoo BK, Ryu JR, Choi EY, Cheong JH, Ryu JH, Ko KH (2003) Induction of matrix metalloproteinase-9 (MMP-9) in lipopolysaccharide-stimulated primary astrocytes is mediated by extracellular signal-regulated protein kinase 1/2 (Erk1/2). *Glia* 41 (1):15-24. doi:10.1002/glia.10131
- Mafficini A, Vezzalini M, Zamai L, Galeotti L, Bergamini G, Della Peruta M, Melotti P, Sorio C (2007) Protein Tyrosine Phosphatase Gamma (PTPgamma) is a Novel Leukocyte Marker Highly Expressed by CD34 Precursors. *Biomark Insights* 2:218-225
- Nishiwaki T, Maeda N, Noda M (1998) Characterization and developmental regulation of proteoglycan-type protein tyrosine phosphatase zeta/RPTPbeta isoforms. *J Biochem* 123 (3):458-467
- Oakley H, Cole SL, Logan S, Maus E, Shao P, Craft J, Guillozet-Bongaarts A, Ohno M, Disterhoft J, Van Eldik L, Berry R, Vassar R (2006) Intraneuronal beta-amyloid aggregates, neurodegeneration, and neuron loss in transgenic mice with five familial

- Alzheimer's disease mutations: potential factors in amyloid plaque formation. *J Neurosci* 26 (40):10129-10140. doi:26/40/10129 [pii]  
10.1523/JNEUROSCI.1202-06.2006
- Reinhard J, Horvat-Brocker A, Illes S, Zaremba A, Knyazev P, Ullrich A, Faissner A (2009) Protein tyrosine phosphatases expression during development of mouse superior colliculus. *Exp Brain Res* 199 (3-4):279-297. doi:10.1007/s00221-009-1963-6
- Romero-Calvo I, Ocon B, Martinez-Moya P, Suarez MD, Zarzuelo A, Martinez-Augustin O, de Medina FS (2010) Reversible Ponceau staining as a loading control alternative to actin in Western blots. *Anal Biochem* 401 (2):318-320. doi:S0003-2697(10)00135-1 [pii]  
10.1016/j.ab.2010.02.036
- Sakurai, T., Friedlander, D. R., & Grumet, M. (1996). Expression of polypeptide variants of receptor-type protein tyrosine phosphatase beta: the secreted form, phosphacan, increases dramatically during embryonic development and modulates glial cell behavior in vitro. [Research Support, Non-U.S. Gov't Research Support, U.S. Gov't, P.H.S.]. *J Neurosci Res*, 43(6), 694-706, doi:10.1002/(SICI)1097-4547(19960315)43:6<694::AID-JNR6>3.0.CO;2-9.
- Sandvig, A., Berry, M., Barrett, L. B., Butt, A., & Logan, A. (2004). Myelin-, reactive glia-, and scar-derived CNS axon growth inhibitors: expression, receptor signaling, and correlation with axon regeneration. [Review]. *Glia*, 46(3), 225-251, doi:10.1002/glia.10315.
- Schumann G, Fiebich BL, Menzel D, Hull M, Butcher R, Nielsen P, Bauer J (1998) Cytokine-induced transcription of protein-tyrosine-phosphatases in human astrocytoma cells. *Brain Res Mol Brain Res* 62 (1):56-64. doi:S0169328X9800237X [pii]
- Shintani T, Maeda N, Nishiwaki T, Noda M (1997) Characterization of rat receptor-like protein tyrosine phosphatase gamma isoforms. *Biochem Biophys Res Commun* 230 (2):419-425. doi:S0006-291X(96)95973-2 [pii]  
10.1006/bbrc.1996.5973
- Shintani T, Maeda N, Noda M (2001) Receptor-like protein tyrosine phosphatase gamma (RPTPgamma), but not PTPzeta/RPTPbeta, inhibits nerve-growth-factor-induced neurite outgrowth in PC12D cells. *Dev Neurosci* 23 (1):55-69. doi:48696 [pii]
- Shintani T, Watanabe E, Maeda N, Noda M (1998) Neurons as well as astrocytes express proteoglycan-type protein tyrosine phosphatase zeta/RPTPbeta: analysis of mice in which the PTPzeta/RPTPbeta gene was replaced with the LacZ gene. *Neurosci Lett* 247 (2-3):135-138

- Sorio C, Mendrola J, Lou Z, LaForgia S, Croce CM, Huebner K (1995) Characterization of the receptor protein tyrosine phosphatase gene product PTP gamma: binding and activation by triphosphorylated nucleosides. *Cancer Res* 55 (21):4855-4864
- Tanaka M, Maeda N, Noda M, Marunouchi T (2003) A chondroitin sulfate proteoglycan PTPzeta /RPTPbeta regulates the morphogenesis of Purkinje cell dendrites in the developing cerebellum. *J Neurosci* 23 (7):2804-2814. doi:23/7/2804 [pii]
- Tonks NK (2006) Protein tyrosine phosphatases: from genes, to function, to disease. *Nat Rev Mol Cell Biol* 7 (11):833-846. doi:nrm2039 [pii]  
10.1038/nrm2039
- Tremblay, M. L. (2009). The PTP family photo album. [Comment]. *Cell*, 136(2), 213-214, doi:10.1016/j.cell.2009.01.006.
- Vezzalini M, Mombello A, Menestrina F, Mafficini A, Della Peruta M, van Niekerk C, Barbareschi M, Scarpa A, Sorio C (2007) Expression of transmembrane protein tyrosine phosphatase gamma (PTPgamma) in normal and neoplastic human tissues. *Histopathology* 50 (5):615-628. doi:HIS2661 [pii]  
10.1111/j.1365-2559.2007.02661.x
- Zhang W, Savelieva K V, Tran D, Pogorelov V M, Cullinan E B, Backer K B, Platt K A, Hu S, Rajan I, Xu N, Lanthorn T H (2012) Characterization of PTPRG in knockdown and phosphatase-inactive mutant mice and substrate trapping analysis of PTPRG in mammalian cells. *Plos One* 7 (9) e45500. doi:10.1371/journal.pone.0045500

Figure 1  
[Click here to download high resolution image](#)

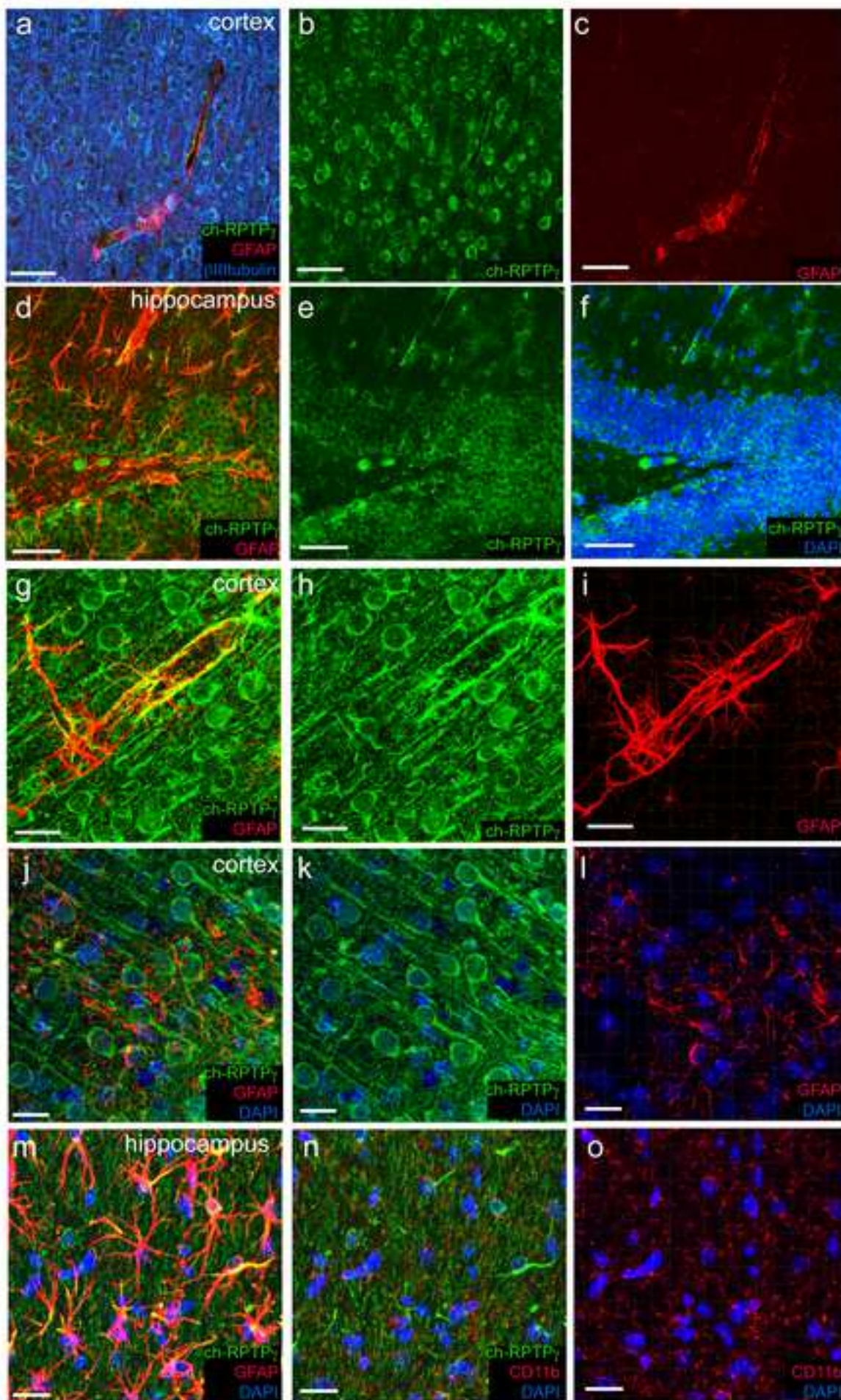


Figure 2  
[Click here to download high resolution image](#)

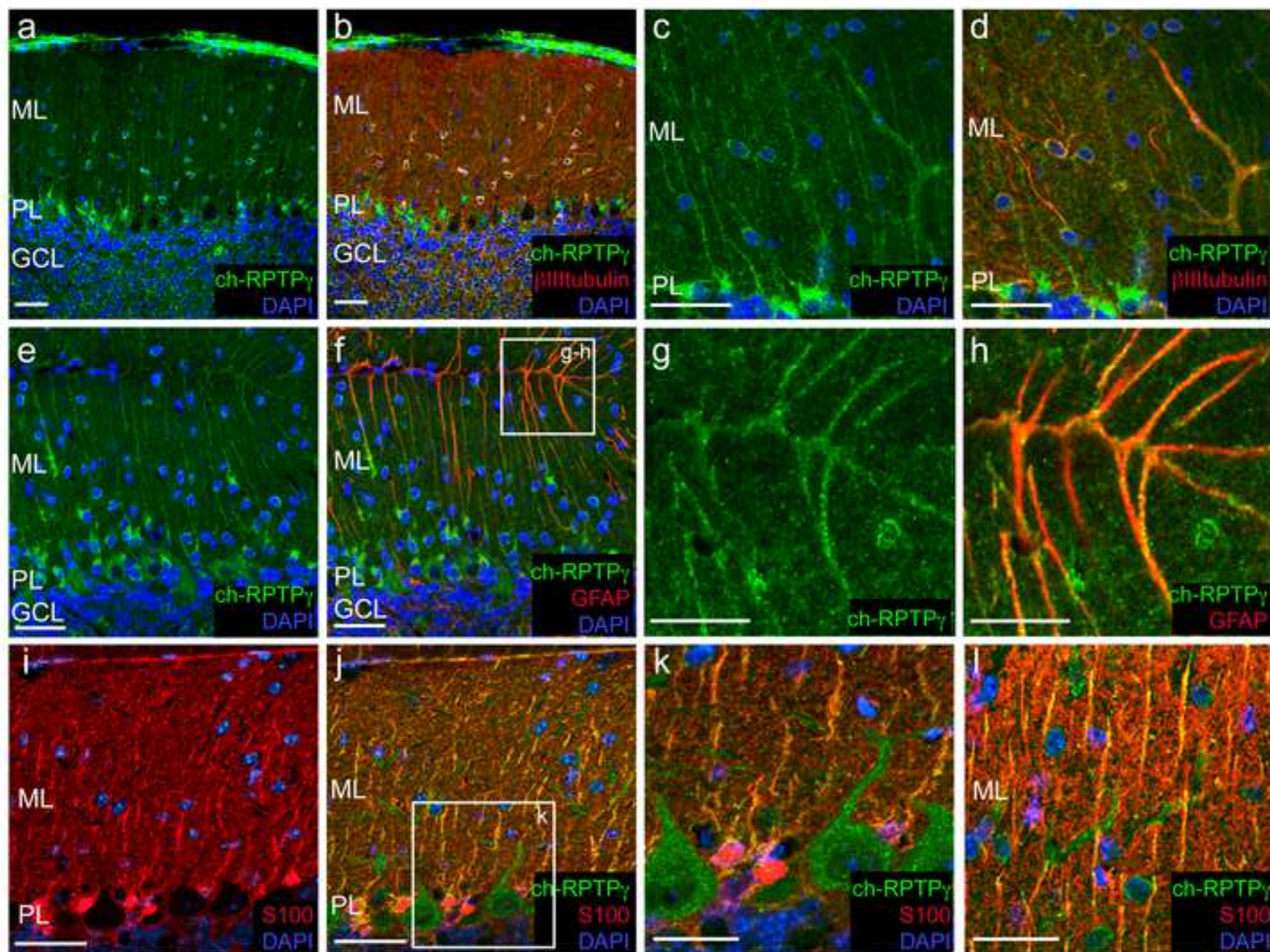


Figure 3  
[Click here to download high resolution image](#)

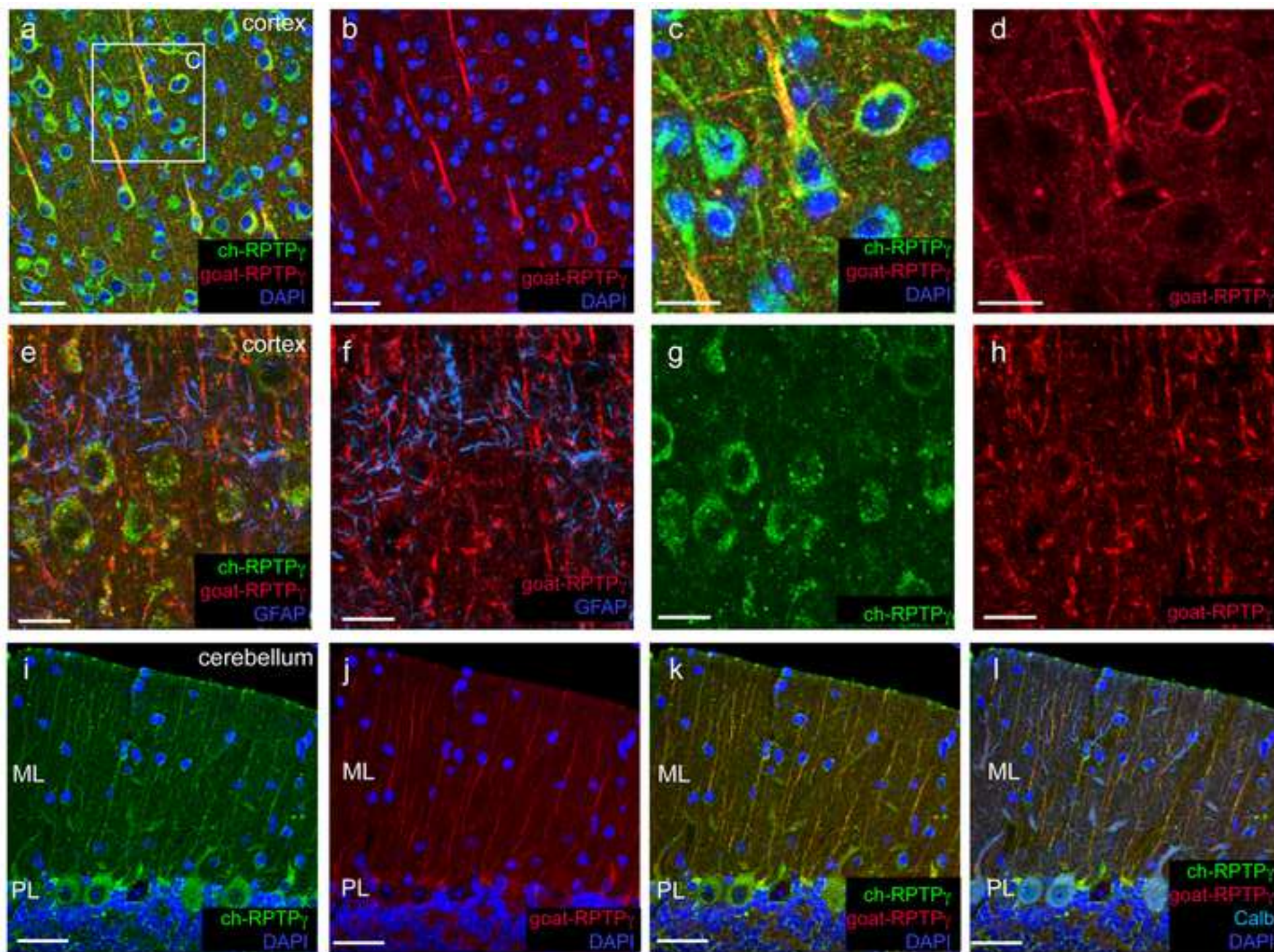


Figure 4  
[Click here to download high resolution image](#)

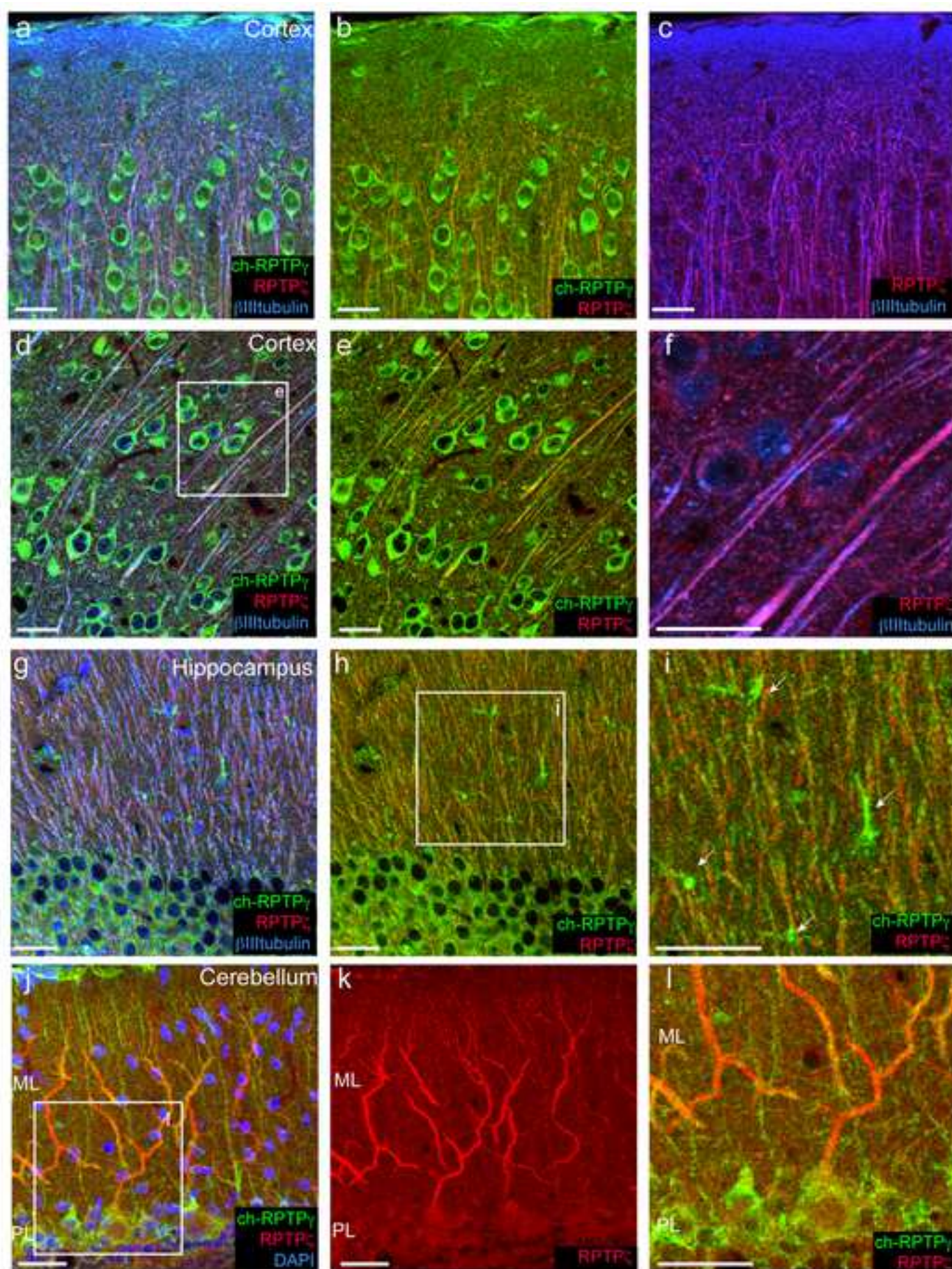


Figure 5  
[Click here to download high resolution image](#)

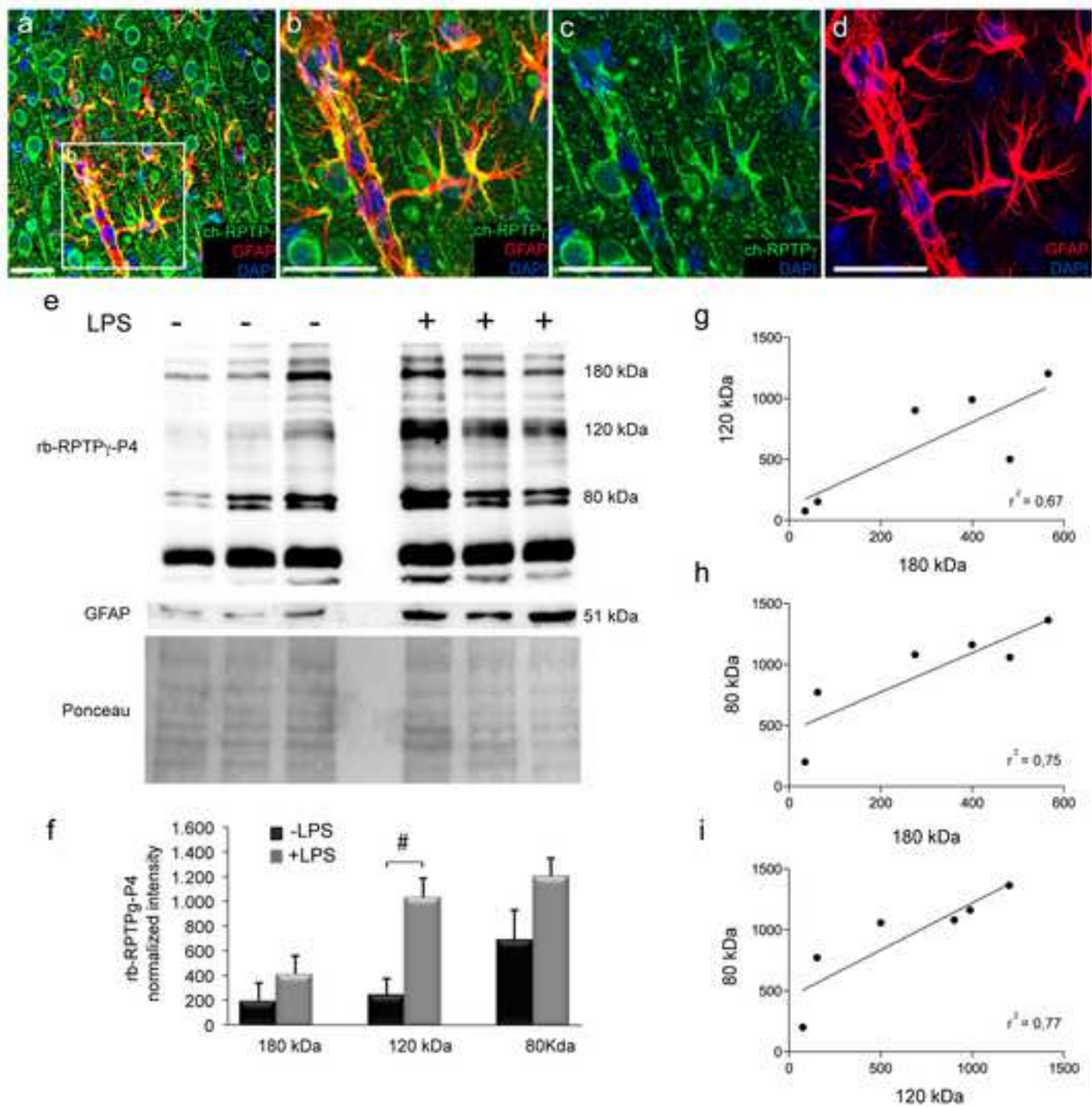


Figure 6  
[Click here to download high resolution image](#)

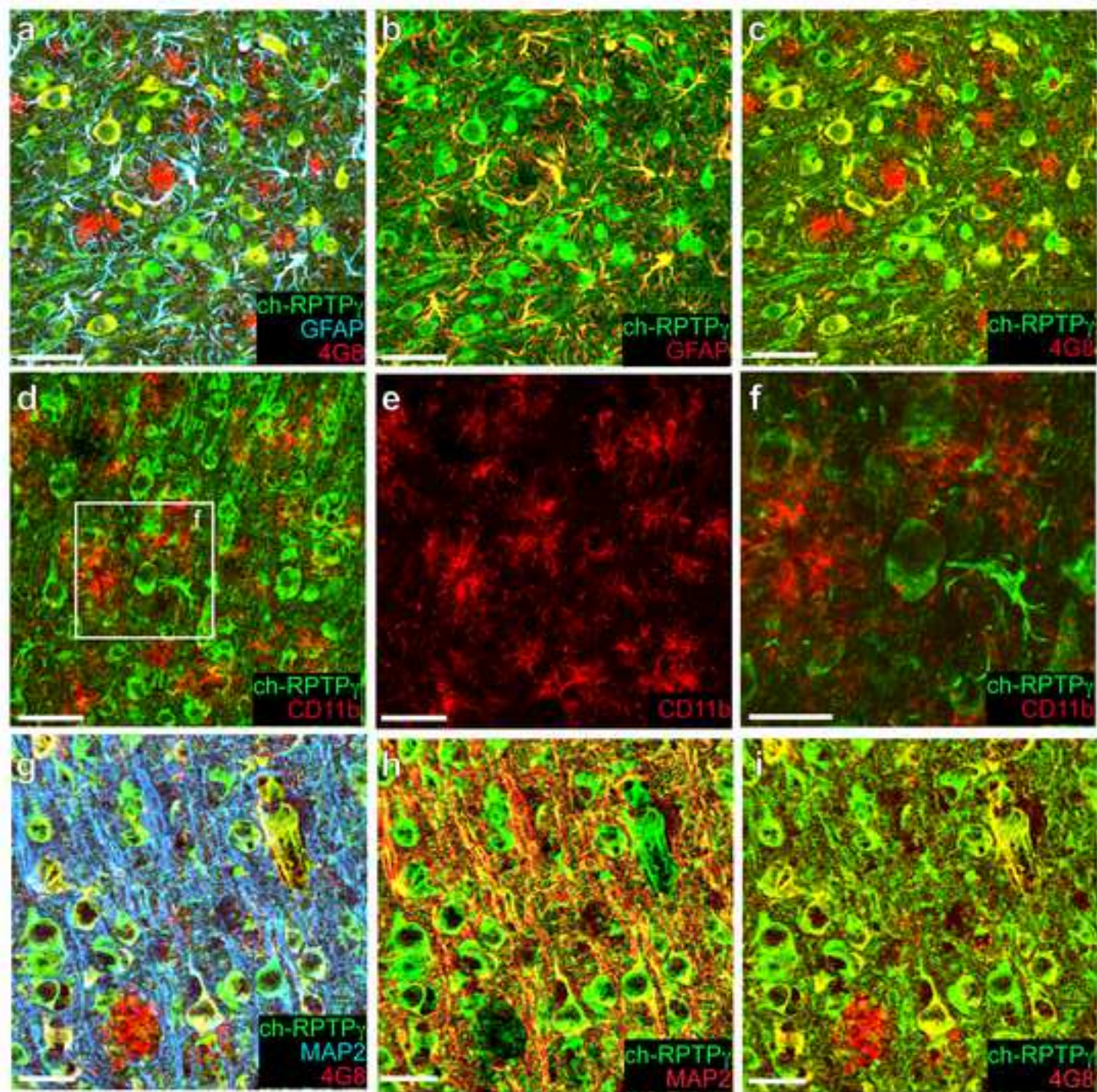
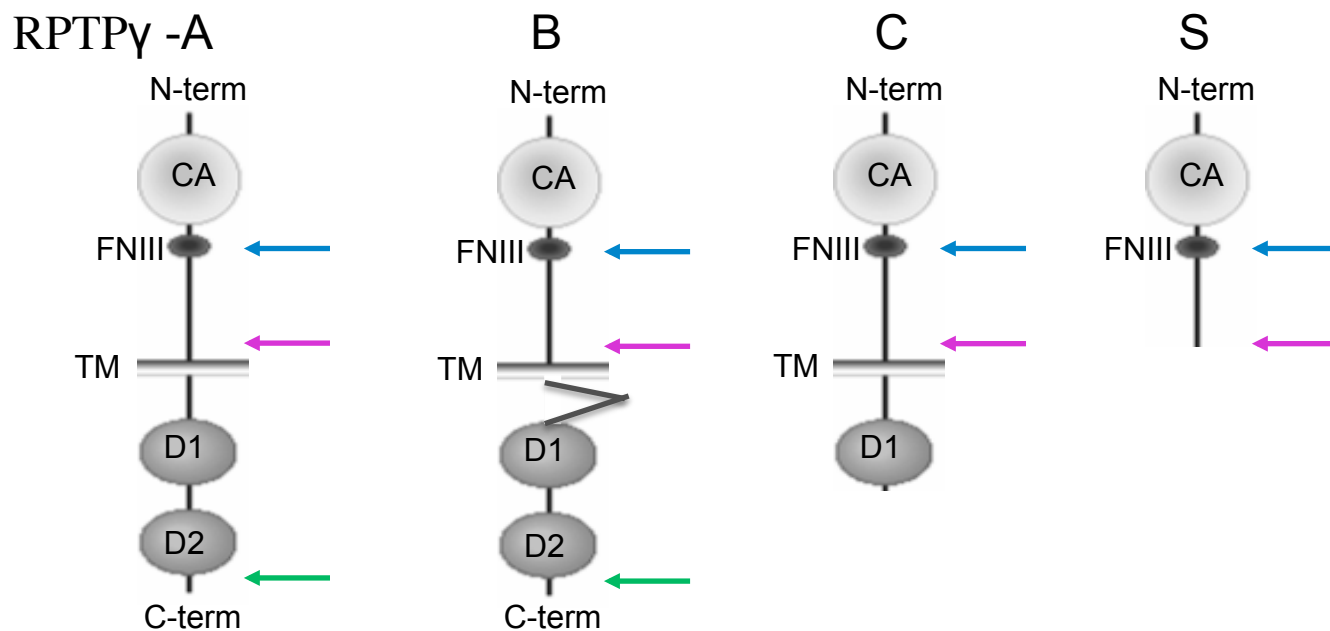


Table 1. Antibodies and schematic localization of epitopes on the different RPTP $\gamma$  isoforms

Antibody	Class	Epitope	Homology human-mouse	Sequence	Validated application
Chicken PTPRG*	IgY	390-408	100%	CZNEDEKEKFTTKDSD KDLK	IP, WB, IHC, Flow
Rabbit PTPRG-P4**	IgG	687-710	96% (h-K / m-R)***	CGSDPKRPEMPSKPK MSRGDRFSED	IP, WB, IHC, Flow
Goat PTPRG (C-18): sc-1111	IgG	C-term	Cross reactivity Human-mouse- rat	SANTA CRUZ BIOTECHNOLOGY, INC.	WB, IF

\* : Mafficini A et al., (2007)  
Biomarker Insights 2:218-225  
\*\* : Sorio C et al., (1995) Cancer  
Res. 55 (21):4855-4864,  
Vezzalini M et al., (2007)  
Histopathology 50 (5):615-628  
\*\*\*: same class substitution:  
human K (Lys)→ mouse R(Arg)



Distribution of RPTP $\gamma$  positivity in mouse brain

	Structure/nucleus	type of positive cells	positivity	cellular localization	
<b>CEREBRAL CORTEX</b>	AC-anterior cingulate cortex	neurons layer 2+3	+++	perisomatic+neuropile	
	CA1 hippocampus	neurons	+++	perisomatic+neuropile	
	CAT-cortico-amygdaloid transition zone		+++	perisomatic+neuropile	
	cc corpus callosum		-		
	DG-hippocampal dentate gyrus	neurons	++	perisomatic+neuropile	
	IG indusium griseum	neurons	++		
	MO-motory I	neurons layer 2+3-5-6	+++	perisomatic+neuropile	
	MO-motory II	neurons layer 2+3-5-6	+++	perisomatic+neuropile	
	PIR-pyriform cortex	neurons layer 2+3	+++	perisomatic+neuropile	
	SFO subfornical organ		+		
	SSP-somatosensory I	neurons layers 2-3-4-5-6	+++	perisomatic+neuropile	
	TRS triangular Nucleus of septum	neurons	++	soma	
	ventral hippocampal commissure	glia	+	perisomatic	
	VISC-visceral cortical area		+++	perisomatic+neuropile	
	<b>THALAMUS</b>	AD anterodorsal nucleus	neurons	+++	soma
		ac anterior commissure		-	
		AM anteromedial nucleus	neurons	+	soma
			small cells	-	
		AV anteroventral nucleus	neurons	+	soma
BLA- basolateral nucleus of amygdala			++	perisomatic+neuropile	
BSTad bed Nu of stria terminalis, anterodorsal		neurons	++	perisomatic+neuropile	
BSTov bed Nu of stria terminalis, oval part		neurons	+++	perisomatic+neuropile	
CEA-central nucleus of amygdala			+++	cytoplasm+neuropile	
CM-central medial Nu			+++	perisomatic+neuropile	
CP striatum		neurons	++	perisomatic	
		small unidentified cells	-		
fi-fimbria			+	maybe some glial cell	
fx fornix			-		
GPI globus pallidus lateralis		neurons	+++	cytoplasm+some dendrites	
		small unidentified cells			
IAM- interanteromedial nu			+++	perisomatic+neuropile	
int internal capsule		glia?	+		
LD laterodorsal nu		neurons	++	soma	
Lsd lateral septum Nu, dorsal		neurons	+++	perisomatic+neuropile	
Lsi lateral septum Nu, intermediate		neurons	++	perisomatic+neuropile	
LSv lateral septum Nu, ventral		neurons	++	perisomatic+neuropile	
MD- mediodorsal Nu		neurons maybe some glial cell	+++	perisomatic	
MEPO median preoptic Nu			-		
MH medial habenula		neurons	+++	cytoplasm	
PVT-periventricular Nu			++		
RE-reuniens Nu			++	perisomatic+neuropile	
RT reticular Nu		neurons	+++	cytoplasm	
		small cells	-		
sm stria medullaris		glia?	+++		
st stria terminalis			-		
VA ventral anterior Nu			+/-		
VAL-ventral anterolateral Nu		neurons	+++	perisomatic+neuropile	
VPL- ventroposterolateral Nu		neurons	+++	perisomatic+neuropile	
XI-xiphoid Nu			-		
<b>HYPOTHALAMUS</b>		AHN-anterior hypothalamic Nu	neurons	++	perisomatic+neuropile
		ARH arcuate Nu	neurons	++	
		AVP anteroventral preoptic Nu		-	
		AVPV anteroventral periventricular Nu		+	
		LHA-lateral hypothalamic area		+	
		lot- lateral olfactory tract		-	some glial cell
		MEAd- medial nu of amygdala	neurons	+++	
		MPNI- medial preoptic nu, lateral		+	
	MPO-medial preoptic area		-		
	opt-optic tract	some glial cells	+/-		
	OT olfactory tubercle	neurons	++		
	PVH periventricular Nu	neurons	++		
	PVH-paraventricular Nu	neurons	+	perisomatic+neuropil	
	RE reuniens Nu	neurons	++		
	SI substantia innominata	neurons	++		
	SO supraoptic Nu	neurons	+++		
	<b>BRAINSTEM</b>	CNgl - coclear Nu, granular layer		+	
		GRN - gigantocellular reticular Nu	neurons	+++	cytoplasm+neuropil
			small unidentified cells	-	
		icp - inferior cerebellar peduncle		+++	axons
IRN - intermediate reticular Nu			+++	cytoplasm+neuropil	
LVN - lateral vestibular Nu		neurons	+++	cytoplasm+neuropil	
		small unidentified cells	+++		
MARN - magnocellular reticular Nu		neurons	+++	cytoplasm+neuropil	
mif - medial longitudinal fasciculus			-		
ml - medial lemniscus			-		
PARN - parvocellular reticular nucleus			+++	cytoplasm+neuropil	
PGRNd - paragigantocellular reticular nucleus dorsal		neurons	+++	cytoplasm+neuropil	
		small unidentified cells	-		
PGRNI - paragigantocellular reticular nucleus		neurons	+++	cytoplasm+neuropil	
		small unidentified cells	-		
PPY - peripyramidal Nu		neurons	+		
		small unidentified cells			
PRP - Nu prepositus		neurons	++	cytoplasm+neuropil	
		small unidentified cells	++		
py - pyramidal tract		small unidentified cells	-	maybe some glial cells	
RM - Nu raphe magnus		neurons	+++	cytoplasm+neuropil	
RPA - Nu raphe pallidus			-		
rust - rubrospinal tract			-		
SPVOdm - spinal Nu of the trigeminal nerve		neurons	+++	cytoplasm+neuropil	
		small unidentified cells	-		
SPVOvl - spinal Nu of the trigeminal nerve		neurons	+++	cytoplasm+neuropil	
		small unidentified cells	-		
spV-spinal tract of trigeminal nerve		small unidentified cells	-		
tb - trapezoid body		small unidentified cells	-		
VCO - ventral coclear nucleus		neurons	+++	cytoplasm+neuropil	
		small unidentified cells			
VII - nu faciale		neurons	+++	cytoplasm+neuropil	
		small unidentified cells	+++		
vs - ventral spinocerebellar tract		-			
vVIII - vestibulo-coclear nerve, vestibular root	small unidentified cells	+	axons		
<b>CEREBELLUM</b>	DN-dentate Nu	neurons	+++	cytoplasm+neuropil	
		small unidentified cells			
	DNp-dentate Nu parvocellular part	neurons	+++	cytoplasm+neuropil	
	FN fastigial Nu	neurons	+++	cytoplasm+neuropil	
		small unidentified cells	-		
	IP-interposit Nu	neurons	+++	cytoplasm+neuropil	
		small unidentified cells			
	SVN-superior vestibular Nu	neurons	+++	cytoplasm+neuropil	
		small unidentified cells			
	VCN-vestibulocerebellar Nu	neurons	+++	cytoplasm+neuropil	
		small unidentified cells			
	Molecular layer	Bergmann glia	+++	cytoplasm+neuropil	
	granule cells		+/-	uncertain	
Purkinje neurons		+	soma and main dendrite		
Interneurons molecular layer		+	soma		

